The Spring 1985 High Precision Baseline Test of the JPL GPS-Based Geodetic System

A Final Report

John M. Davidson
Catherine L. Thornton
Scott A. Stephens
Geoffrey Blewitt
Stephen M. Lichten
Ojars J. Sovers
Peter M. Kroger
Lisa L. Skrumeda
James S. Border
Ruth E. Neilan
Charles J. Vegos
Bobby G. Williams
Jeffrey T. Freymueller
Timothy H. Dixon
William G. Melbourne

November 15, 1987

The Spring 1985 High Precision Baseline Test of the JPL GPS-Based Geodetic System

A Final Report

John M. Davidson
Catherine L. Thornton
Scott A. Stephens
Geoffrey Blewitt
Stephen M. Lichten
Ojars J. Sovers
Peter M. Kroger
Lisa L. Skrumeda
James S. Border
Ruth E. Neilan
Charles J. Vegos
Bobby G. Williams
Jeffrey T. Freymueller
Timothy H. Dixon
William G. Melbourne

November 15, 1987

PREFACE

During the years 1979 to 1983, JPL conducted a feasibility study to examine the use of the NAVSTAR satellites of the Global Positioning System (GPS) as microwave radio sources for precise geodetic measurements in lieu of compact radio sources distributed throughout the universe. The work was funded by NASA.

In 1984, Congress mandated NASA to establish a civilian geodynamics activity in the Caribbean. JPL, having demonstrated the feasibility and affordability of instrumentation based on using the Global Positioning System, was assigned the responsibility of implementation and early deployment in the Caribbean of this space-oriented geodetic system. It was expected that this capability would provide densification requirements necessary for intensive study of regional deformation at the tectonic plate boundaries. After an intensive and extensive study of the existing positional and navigational instrumentation, JPL arrived at the appropriate system design necessary to achieve accuracies of at least 1 part in 100 million. Soon thereafter, JPL organized a measurement session, using most of the available data acquisition receivers to establish the state-of-the-art. From the onset of this program, it was obvious that NASA could not muster the resources to implement and operate this capability. Therefore, JPL called on universities and agencies, all of which were vitally interested in the outcome of this instrumentation, to cooperate in meeting the objectives of this project. This report presents the findings of the first measurement sessions, conducted in March of 1985. We are pleased to report that we achieved an outstanding collaborative activity which we expect will carry us throughout the next several years. As of the

date of this document, we are preparing a report of the second measurement

session, conducted with the cooperation of the Mexican agencies in Baja

California. Field operations for this second session were conducted in

November of 1985.

M A Renzetti

N. A. Renzetti, Manager

JPL Geodynamics Program

ACKNOWLEDGMENT

We also acknowledge with thanks the long-term support of NASA managers Mr. T. L. Fischetti, Dr. E. A. Flinn and Dr. S. G. Tilford.

$1-2 : 10^7$ in all coordinates, independent of baseline length. The results for baseline repeatability are consistent with the current GPS error budget, but the GPS-VLBI intercomparisons disagree at a somewhat larger level than expected. We hypothesize that these differences may result from errors in the local survey measurements used to correct for the separations of the GPS and VLBI antenna reference centers.

ABSTRACT

The Spring 1985 High Precision Baseline Test (HPBT) of the JPL GPS-Based

Geodetic Measuring System was conducted between March 28, 1985, and April 5,

1985. It involved over a dozen collaborating institutions, with organization

and coordination under NASA/JPL leadership, and was designed to meet a number

of objectives. Foremost among these was the demonstration of a level of

accuracy of $1-2:10^7$, or better, for baselines ranging in length up to several

hundreds of kilometers. In addition, the HPBT was designed to meet a number

of secondary objectives, including the development of efficient procedures for

planning and coordinating large-scale GPS field exercises, the establishment

of institutional interfaces for future cooperative ventures, the initiation of

a series of calibration measurements on well-determined VLBI baselines, the

testing of the GPS data analysis software and analysis procedures, and an

initial site occupation designed to monitor uplift in the Long Valley caldera

region near Mammoth Lakes, California.

These objectives were all met with a high degree of success, with respect

to the demonstration of system accuracy in particular. The results from six

baselines ranging in length from 70 to 729 km were examined for repeatability

and, in the case of three baselines, were compared to results from colocated

VLBI systems. Repeatability was found to be $5:10^8$ (RMS) for the north

baseline coordinate, independent of baseline length, while for the east

coordinate RMS repeatability was found to be larger than this by factors of

2-4. The GPS-based results were found to be in agreement with those from

colocated VLBI measurements, when corrected for the physical separations of

the VLBI and GPS antennas (typically on the order of 0.5 km), at the level of

CONTENTS

List of Tables

List of Figures

CONTENTS (Continued)

I. Introduction

Over the past fifteen years, the space geodetic techniques of satellite laser ranging (SLR) and very long baseline interferometry (VLBI) have been applied to the measurement of earth orientation and global crustal motion [e.g., Herring et al., 1986; Christodoulidis et al., 1985; Davidson and Trask, 1985; Kroger et al., 1987; Sovers et al., 1984]. The results from these and other studies are generally consistent with those inferred for geologic time spans [Minster and Jordan, 1978]. However, the low resolution provided by the sparse VLBI and SLR networks provides a strong incentive for network densification. Increased resolution is particularly motivated near tectonic plate boundaries, where extensive, non-uniform, and possibly time-varying strain fields may exist.

Geodetic systems utilizing signals from the Global Positioning System (GPS) satellites have long been recognized as holding the key to such densification [e.g., Melbourne et al., 1986]. These satellites broadcast phase-modulated signals at two L-band frequencies (1575.41 MHz and 1227.60 MHz) and have already attracted many civilian users for applications in navigation, precise orbiter tracking and geodesy. The intensity of the GPS satellite signals--up to 10^8 times that of the natural radio sources typically used in VLBI geodesy--has led to the development of GPS-based geodetic receivers which are relatively transportable, inexpensive, and easy to operate [e.g., Crow et al., 1984; Block et al., 1985]. In parallel with this, large software systems have been developed at JPL, and other centers, for analysis of GPS geodetic data.

A test of these systems in the regional context (i.e., involving baselines of up to several hundred kilometers in length) was conducted under NASA/Jet Propulsion Laboratory (JPL) leadership in the Spring of 1985. The principal objective of this test was the demonstration of geodetic quality accuracy for the total GPS system, including satellite constellation, field equipment, and data analysis software and procedures. In principle, the accuracy of GPS-based systems may eventually rival that already attained by VLBI-based systems, where differential positioning accuracies of $1:10^8$, or better, are now routinely attained. However, for purposes of this test, an initial goal of $1-2:10^7$ was set. This will establish the sensitivity of the GPS systems to expected regional deformation rates of 3-5 cm/yr, for monitoring programs spanning no more than several years. In this work, we will show that this goal was achieved for baselines ranging from 70 to 729 km in length.

II. The Spring 1985 High Precision Baseline Test

Objectives of the Test

The Spring 1985 High Precision Baseline Test (HPBT) involved over a dozen collaborating institutions (Table 1) and was organized and coordinated by NASA/ JPL. The test was designed to meet a number of objectives. Foremost among these was the demonstration of a level of accuracy of $1-2:10^7$, or better. Central to the achievement of this accuracy goal is the fiducial network approach for high-accuracy GPS-based geodesy, which is discussed in detail in Section III. Other major objectives of the HPBT included the development of efficient procedures for planning and coordinating large-scale GPS field exercises, the establishment of institutional interfaces for future cooperative

ventures, the initiation of a series of calibration measurements on well-determined VLBI baselines, the testing of the GPS data analysis software and analysis procedures, and an initial site occupation designed to monitor uplift in the Long Valley caldera region near Mammoth Lakes, California. In addition, this test was designed to permit an assessment of the performance of the participating GPS receiver types and facilitate the testing of water vapor radiometers (WVRs) for the calibration of GPS data.

Criteria for Site Selection

In the HPBT, a total of fifteen receivers were deployed to ten sites across the United States. These sites fell into four classes: fiducial sites (see Section III), mobile calibration sites, other mobile sites and one scientifically motivated site. One site served in two of these roles. In the selection of the fiducial site locations, the VLBI stations of the NOAA/NGS POLARIS Project were chosen, with sites located near Westford, MA; Richmond, FL; and Ft. Davis, TX. In addition, a fourth fiducial receiver was located at the Owens Valley Radio Observatory (OVRO) near Big Pine, CA. In the selection of the mobile calibration sites, it was necessary to choose VLBI observatories whose positions were accurately measured with respect to fiducial network, so that the GPS-based results could be compared with those based on colocated VLBI measurements. Accordingly, sites at the Mojave VLBI station of the NASA Crustal Dynamics Project, near Barstow, CA; the Owens Valley Radio Observatory; and the Hat Creek Radio Observatory, near Hat Creek, CA, were selected as the endpoints for the calibration baselines. Other mobile GPS receivers, belonging to various of the collaborating institutions, recorded data during the HPBT. These were not located at sites of either well-established a priori location or

3

of scientific interest and are not treated further in this work. They include receivers located at Pt. Mugu, CA; Austin, TX; and Dahlgren, VA.

To demonstrate the applicability of GPS-based geodesy to a scientific problem of current interest, one mobile receiver was deployed to a site near Mammoth Lakes, CA, to investigate ground deformation in the Long Valley caldera region. This site was established as part of a JPL-Caltech program designed to supplement ongoing geodetic measurements by the U.S. Geological Survey (USGS). Part of the USGS program consists of leveling surveys, designed to monitor vertical motion associated with the uplift of a resurgent dome in the Long Valley caldera. This is thought to be due to the intrusion of magma into a shallow ($\leq$ 10 km depth) crustal reservoir [Savage and Clark, 1982; Rundle and Whitcomb, 1984], and represents a potential volcanic hazard. A detailed analysis and discussion of the results from the occupation of the Long Valley site will be presented in a separate report.

Description of Field Operations

The Spring 1985 HPBT took place between March 28, 1985, and April 5, 1985. Fifteen GPS receivers were placed at ten sites as described in the preceding subsections. These ten sites were equipped with a variety of GPS receiver types, including SERIES-X [Crow et al., 1984], TI-4100 [Henson et al., 1985] and Air Force Geophysical Laboratories (AFGL) dual-frequency receivers [Ladd and Counselman, 1985]. Frequency standards used in different phases of the test included hydrogen masers, Rb clocks and quartz crystal clocks. Three of the sites in California were instrumented with WVRs. A summary of receiver, clock and WVR deployment information is given in Table 2. As of late March 1985, the GPS constellation was configured so that it came together over North

America once per sidereal day, remaining above any local horizon for approximately six hours. The satellite configuration, or geometry, was virtually identical from day to day. In California at that time, this six hour view period began at approximately 04:00 GMT (8:00 p.m. Pacific Standard Time). The dates on which sessions were successfully conducted include the six days from March 31, 1985, through April 5, 1985. A map showing the locations of the receivers deployed in this test is presented in Figure 1.

III. The Fiducial Network Concept

Unification of the GPS and VLBI Coordinate Systems

The accuracy of GPS-based measurements depends in large part on the accuracies with which the GPS satellite orbits have been determined. Currently available post-fit ephemerides define a self-consistent frame of reference at the level of approximately $1:10^6$. Given expected rates of crustal motion of ≤ 5 cm/yr, a geodetic measurement program relying on post-fit ephemerides, and requiring temporal resolution of less than a decade, would be sensitive to such motions over distances of no more than several tens of km. On the other hand, a reference system relying on VLBI or SLR measurements to establish and maintain coordinate system orientation and scaling is potentially self-consistent at a level of $1:10^8$ or better. Hence, a GPS network tied to the VLBI coordinate system could be utilized for geodetic measurement on a regional scale, or greater.

A means of establishing this frame tie and improving the accuracy of the GPS ephemeris—and hence of GPS-based baseline measurements—has been actively pursued at JPL and is known as the fiducial network approach. In this

5

approach, three or more receivers are placed at locations, called fiducial sites, whose positions have been well-established by VLBI. Additional receivers, known as mobile receivers, are placed at sites of geodetic interest. The fiducial network must be well extended in both latitude and longitude, and should be of a scale size somewhat larger than that of the mobile receiver network. During a GPS-based measurement, the fiducial receivers record data jointly with the mobile receivers, enabling simultaneous determination of accurate GPS satellite orbits and geodetic baselines. To the extent that orbital dynamics, clocks and atmospheric effects are adequately modeled, the accuracy of the mobile receiver locations will reflect that of the fiducial receiver locations to which they are referenced.

It should be noted that by locating the fiducial receivers at VLBI stations, the GPS orbit and baseline solutions are inherently expressed in the coordinate system of the extragalactic radio sources. This has the aesthetic appeal of unifying the GPS and VLBI results in an inertial, or absolute, frame of reference and has the practical benefits of permitting their simultaneous display, direct comparison and combined use in geophysical interpretation. A schematic illustration of the fiducial network method for accurate GPS-based geodesy is shown in Figure 2.

Covariance Analysis Results

In earlier considerations of the fiducial approach to GPS-based geodesy, and in designing the Spring 1985 HPBT, covariance analyses were performed to predict system performance for the baselines to be occupied. Figure 3 summarizes the covariance analysis results for one of these baselines, the 245 km Mojave/Owens Valley baseline [Davidson et al., 1985], based on the actual

observing scenario that had been planned for the HPBT. This scenario involved one continuous observing session of six hours, with observations recorded every six minutes. The error model assumptions were as follows. Zenith troposphere calibration accuracy was taken to be 2 cm at stations where WVR data were taken and 5 cm otherwise; fiducial baseline accuracy was taken to be 3 cm in all coordinates; a priori satellite position and velocity at epoch were taken to be 10 m and 1 mm/sec, respectively; uncertainty in geocenter location was taken to be 20 cm in all coordinates; modeling of solar radiation pressure on the GPS spacecraft was assumed to be accurate to within 5% of the total effect; the value of GM was taken to be accurate to $1:10^8$; the error in the gravity model was taken to be 50% of the difference between the GEM6 and the APL5.0 gravity models; the elevation angle cutoff at each station was taken to be 15 degrees; the data type used was carrier phase (i.e., integrated doppler); and data noise was taken to be 2 cm. These error model assumptions were the standard ones used for the systems to be deployed in the HPBT and their validity was borne out in the analysis of experimental data several months later. Two covariance analyses based on the observing plan of the HPBT were made, one in which the satellite epoch states were estimated (i.e., using the fiducial network approach) and one in which they were fixed at their a priori values (i.e., as if it were a two-station experiment with no fiducial network and no orbit estimation). An intermediate case in which satellite orbits were estimated, but in which none of the GPS receivers had well-established a priori locations (i.e., a free network solution in which all stations were mobile stations), gives results between the two extremes shown in Figure 3. As this figure shows, the use of a fiducial network and orbit estimation is expected to improve accuracy for this baseline by factors of from five in the vertical

to forty in the north. As we shall see, this prediction via covariance
analysis of system performance in the HPBT was borne out in the results from
the actual HPBT data.

IV. Data Analysis

The GIPSY Software

The GIPSY (GPS Inferred Positioning SYstem) software for GPS data analysis
was developed at JPL between January 1985 and the present. It consists of over
70,000 lines of code, approximately one-third of which were adapted from pre-
existing software systems, such as the VLBI data analysis code MASTERFIT
[Sovers and Fanselow, 1986] and the spacecraft orbital dynamics modeling code
Double Precision Trajectory Program (DPTRAJ) [Moyer, 1971]. The remaining
two-thirds consist of newly written code, much of which is also used in the
OASIS (Orbit Analysis SImulation System) covariance analysis software system
[Wu and Thornton, 1985]. Briefly, GIPSY consists of: a comprehensive front
end for data editing, phase connection, atmospheric calibrations and data
compression; FESCHED, an experiment scheduling program which generates
observing schedules, rise-set tables and plots, satellite ground and sky
tracks, and artificial data for covariance analysis; PATH-VARY, a program
which generates satellite trajectories and integrates variational equations to
form transition matrices for satellite states and dynamic model parameters;
GPSOMC (observed minus calculated), which computes an accurate model
observable and pre-fit residuals; OAFILTER, a U $-$ D factorized batch
sequential process noise filter to do parameter estimation and covariance
analysis; and an output processor to display orbits, baselines and parameter
solutions and covariances. Model accuracy in GIPSY is believed to be better

8

than 1 cm. GIPSY has a number of flexible clock modeling options, including white (uncorrelated) or colored process noise, which, in the case of white noise, is analogous to (though more general than) double differencing, and representation as polynomials of degree one or two over specified data arcs. In addition, singly or doubly differenced observables can be explicitly generated. The software is capable of combining data from different receiver types and of processing different data types (e.g., carrier phase and pseudorange) simultaneously. Estimated and considered (see Section VI) parameters may include satellite position and velocity at epoch, station position and velocity, station and satellite clocks, range biases (for carrier phase data), three solar radiation coefficients for each satellite, zenith tropospheric delay, rate-of-change, and mapping parameters at each station, earth orientation parameters, corrections to precession and nutation, geocenter coordinates, solid earth tide Love numbers and tidal phase, coordinate scale error, and the general relativity γ-factor of the Brans-Dicke theory. (It should be noted that in current processing, especially involving data arcs of six hours or less, only a subset of these parameters is estimated.) The GIPSY software is written in FORTRAN and runs on any of the VAX 11/700 or 8000 series or on the new MicroVAX II series, running under the VMS version 4.4 (or higher) operating system. Detailed mathematical descriptions of the model observables and partial derivatives generated in the OMC module are presented in a separate report [Sovers and Border, 1987]. Mathematical descriptions of the operations performed by the OAFILTER module have been given by Bierman [1977] and Wu et al. [1986].

A Priori Receiver Coordinates

The VLBI-based baseline solutions used to establish the coordinates of the fiducial and calibration sites in a consistent reference frame were those of global solution S284C of Ryan and Ma [1985]. The quoted formal uncertainties in three dimensions for these coordinates range from slightly less than 1 cm to slightly less than 2 cm. In addition, an unimplemented relativity correction in the model calculations of the VLBI data analysis software used by those authors has introduced a scale error of approximately $1.4:10^8$ in the fiducial baseline length estimates reported in that work.

The local survey measurements used to relate the VLBI antenna intersection of axes to local survey monuments (invariably within 1 km of the VLBI antenna) were taken from the Crustal Dynamics Project: Catalogue of Site Information [NASA, 1983]. The precision of these survey measurements is quoted in that reference as being "subcentimeter," but it is noted further that their true accuracy may be somewhat worse, owing to distortions in the NAD27 coordinate system, in which the local surveys were made. However, we claim that undetected errors on the order of 4 cm may persist in the local survey data. We base this conjecture on two facts. First, two significant survey errors were discovered in the course of the present work, one of 20 cm at Ft. Davis by R. W. King [personal communication, 1986] and one of 35 cm at OVRO by the authors. Second, observed systematic differences between VLBI and GPS measurements occur at about this level on a number of baselines in such a way as to indicate local survey error as a possible explanation. This evidence is presented and discussed in Section V.

The GPS antenna site vectors, relating a reference point on the antenna to a nearby monument (usually directly beneath the antenna by a distance of

1-2 m), are measured in the field by receiver operators. The precision of these relatively simple measurements is on the order of 0.2 cm. The locations of the separate L1 and L2 phase centers with respect to this reference point were taken from Sims [1985]. In that work, it is also shown that the measured locations of the L1 and L2 reference points of the TI-4100 antennas differ by up to 1 cm between different antennas and there are phase variations as a function of satellite elevation and azimuth at about that level. In addition, phase center locations may suffer effective shifts in location owing to reflections (i.e., multipathing; see Section VI) from nearby surfaces. These effects limit site vector accuracy for these antennas to approximately 1 cm. Similar shifts may occur in the cases of the SERIES-X and AFGL antennas, but they have not been well-studied or documented, and we make no attempt to quantify them here. For purposes of error assessment in this work, we make the assumption that the size of these effects for these antennas is similar to that reported for the TI-4100 antenna.

A correction for the offset of the origin of the VLBI coordinate system from the geocenter was made, based on a least-squares fit of colocation data from four sites to determine offset-of-origin and rotation of the VLBI and SLR coordinate frames [R. W. King, personal communication, 1986]. The estimated size of this offset in meters (SLR - VLBI) is 1.752, -1.179 and 0.304 in geocentric x, y and z, respectively. The accuracy of this correction is taken to be 10 cm [Smith et al., 1985; Tapley et al., 1985].

We do not expect temporal baseline changes from crustal deformation to be a significant source of error for the fiducial and mobile calibration baselines involved in this work, because they all lie within the North American plate.

Repeated VLBI measurement of these baselines spanning many years limits uncertainty in station location from this error source to approximately 1 cm [Herring et al., 1986].

Geocentric coordinates used in this work for the reference monuments over which the fiducial and mobile calibration GPS receivers were placed are given in Table 3; site vectors connecting reference monuments to antenna phase centers are given in Table 4; and monument identification information is given in Table 5.

A Priori Satellite Ephemeris

The nominal orbits used in this work to initialize the parameter estimation were based on the precise ephemeris provided to us by the Naval Surface Weapons Center (NSWC). The NSWC orbits at that time were computed in the WGS-72 coordinate system, with reference epoch A1950.0, from a one-week fit (plus a one-week prediction) and are thought to be internally consistent at the level of 15-20 meters. Because the coordinates of the fiducial sites used in this work are expressed in the VLBI coordinate system, with reference epoch J2000.0, it was decided to transform the NSWC orbits to correct for the large difference between the two reference epoch definitions, before they were used to initialize data processing. In addition, they were scaled to account for the different values of GM used in the NSWC and GIPSY software systems. The remaining difference between the two coordinate systems consisted mainly of a fairly large offset in longitude. Previously published values for this offset range from 0.5 to 0.8 arcsec [Hothem et al., 1982]. An estimation from the Spring 1985 HPBT data itself has been made by Lichten et al. [1986], who report a value of 0.68 arcsec (3.3 µrad) in UT1 - UTC, consistent with the

12

earlier report. Rotations about the x- and y-axes were estimated to be smaller by over an order of magnitude.

Atmospheric Calibrations

Removal of propagation media distortions was done essentially as has been done in VLBI-based geodesy (which is also a microwave-based technique) for a number of years [e.g., Davidson and Trask, 1985]. Briefly, the techniques used were as follows. Removal of ionosphere effects was based on an assumed inverse-squared frequency dependence for ionosphere dispersion, with carrier phase data, recorded simultaneously at the L1 and L2 frequencies (1575.41 MHz and 1227.60 MHz), combined to create ionosphere-free observables. Calibration of the dry troposphere at the local zenith was obtained directly from the surface barometric pressure; mapping of the dry air mass from the zenith to the satellite line-of-sight was done using the mapping algorithm of Lanyi [1984]. Calibration of the zenith wet troposphere was obtained from WVR data, when that was available, and otherwise from surface meteorology (SM) data used as input to atmospheric models. The reduction of WVR data was according to the algorithm of Robinson [1986] and the reduction of the SM data used the algorithm of Chao [1973]. Mapping of the wet troposphere delay to the satellite line-of-sight was also done as per Lanyi [1984]. The accuracy at zenith of these combined troposphere calibrations was taken to be 2 cm and 6 cm, for WVR and SM data, respectively, with the exception of the calibrations based on the DSN prototype WVR located at Hat Creek, CA (Table 2). Calibrations based on this WVR were assigned an uncertainty of 6 cm, based on the behavior in initial parameter adjustments of the estimated additive constant delay at zenith and on the fact that this WVR is an early prototype known to have relatively large instrumental instabilities.

13

Estimation of Parameters

In our initial processing, we focused on a representative subset of the HPBT data. This subset consisted of the carrier phase data from the AFGL receivers located at the POLARIS VLBI sites (see Section II); the SERIES-X receivers located at Mojave and OVRO; the TI-4100 receivers located at Mojave, OVRO, Mammoth Lakes and Hat Creek; and observing GPS satellites GPS 1, GPS 3, GPS 4, GPS 6, GPS 8, GPS 9 and GPS 10 (launch sequence numbers). Pseudorange data were not used because of the high level of multipath error. (See Section VI.) Data were processed separately for each of the 6 hour sessions on March 31, 1985, through April 5, 1985. Estimated parameters included satellite positions and velocities at epoch, a separate constant correction at all stations to the zenith troposphere delay, mobile station coordinates, station and spacecraft clock offsets, and range biases. Uncertainties in unestimated parameters included in the computation of covariances include uncertainties in fiducial station coordinates, geocenter coordinates, solar radiation parameters, coordinate scale, and earth orientation parameters. The stations treated as mobile stations in the parameter estimation included the SERIES-X receiver at Mojave and the TI-4199 receivers at Mojave, OVRO, Hat Creek and Mammoth Lakes. The stations treated as fiducial receivers included the SERIES-X receiver at OVRO and the AFGL receivers at the POLARIS VLBI sites. Clock offsets were treated as stochastic parameters, with a white noise error model, which is equivalent to clock removal via explicit double-differencing. Data noise was adjusted to attain a χ^2 per degree of freedom of unity. This noise, or weighting, was initially adjusted separately for each receiver type, based on the RMS scatter of post-fit residuals; however, RMS scatter was found to lie consistently in the range 7-8 mm, independent of receiver type. Hence,

a uniform data noise was adopted for all carrier phase observables. The data

noise adopted was 1.0 cm for all six sessions. A summary of estimated and

considered parameters and their a priori uncertainties is given in Table 6.

V. Results

Estimated Parameters and Covariances

Baseline results for each of the six days from March 31, 1985, through

April 5, 1985 are given in Table 7. (For some baselines, station outages have

reduced the number of daily solutions to five or four.) This table gives the

offsets of the GPS-based daily solutions from the VLBI-based a priori baseline

values (see Table 5), with the sign sense being: offset=solution-a priori.

Two uncertainties are given in Table 7 for each daily solution: a formal

standard error and a total absolute error. These differ in that the latter

includes contributions from several important systematic error sources,

including errors in fiducial position, earth orientation, coordinate scale,

solar radiation pressure modeling, and geocenter location. Also given for

each baseline component are: the weighted mean value of the daily solutions;

the weighted RMS scatter about the mean; and the χ^2 per degree of freedom

in calculating the mean. The weights used in computing the mean values are

the inverse squares of the formal standard errors of the daily solutions. Two

uncertainties are given for each mean value. These correspond to those given

for the daily solutions, with the formal standard error of the mean given by

$RMS/\sqrt{N-1}$ and with the total absolute error of the mean (as with the daily

solutions) including contributions from systematic error sources. In the case

of the total absolute error of the mean, an additional error contribution of

4 cm accounting for mobile site survey error is quadratically summed to the systematic error contributions listed above. A quantitative discussion of these error sources is presented in the following section.

Baseline Repeatability

Day-to-day repeatability of estimated baseline components defines measurement precision, provides a lower limit on system inherent accuracy and can give important insight into system performance. Values of RMS repeatability are given in Table 7 for all eight baselines connecting the receivers at the Mojave, OVRO and Hat Creek sites. A plot showing typical results in the horizontal plane is given in Figure 4 for the 245 km length OVRO/Mojave baseline between the two SERIES-X receivers. Repeatability about the mean in the north is 0.6 cm (RMS), or $3:10^8$, while in the east it is $1:10^7$. In the case of the north component, this repeatability approaches that attained for mobile VLBI measurements for baselines of this length [Davidson and Trask, 1985; Kroger et al., 1987]. When the north repeatability is examined for all of the baselines between GPS receivers located in California, including those involving the receiver located near Mammoth Lakes, it is seen to be a strong function of length, being very close to $5:10^8$ for all baselines, with lengths ranging from 70 km to 729 km (Figure 5). For the case of the east and vertical components, the day-to-day repeatability taken over all baselines is uncorrelated with length and falls in the range $1-2:10^7$. These results meet the accuracy objectives set for the Spring 1985 Test (see Section I) and represent a level of system performance which would provide sensitivity to expected regional deformation rates for geodetic monitoring programs spanning only several years. The causes of the larger day-to-day scatter in the east and

vertical, as opposed to the north, and the prospects for $1:10^8$ precision in all components are discussed in Section VI.

Comparison of GPS and VLBI Baselines

Comparison of GPS measurements with results from an independent technique of comparable accuracy, such as VLBI, provides an additional test of GPS system absolute accuracy. In this subsection, we compare GPS and VLBI results for the eight baselines (length > 1 km) connecting the five GPS receivers located at the Mojave, OVRO and Hat Creek VLBI sites. (See Table 2.) From Table 7 and Figure 4, we see that the colocated GPS and VLBI baseline measurements typically differ in the horizontal plane by 5 cm, with differences in some cases ranging up to 10 cm. When these differences are plotted for all eight baselines, a systematic pattern appears. Figure 6 shows the weighted averages of the single-day solutions for March 31, 1985, through April 5, 1985 for each of the eight baselines. In this figure, we see that while all four of the Mojave/ OVRO baselines differ from the VLBI measurement by about 8 cm, they agree with each other within the measurement precision, as defined by the RMS repeatability for each individual baseline (Table 7). This is especially true in the case of the better-determined north baseline components, for which the agreement among these four baselines is better than 1 cm. Similar conclusions may be drawn regarding the two Hat Creek/OVRO baselines and the two Mojave/Hat Creek baselines. This highly systematic grouping by baseline of GPS/VLBI differences strongly suggests the presence of errors on the order of 4 cm in the local (length < 1 km) surveys which are used to correct for the physical separations of the VLBI antenna reference point (the intersection of the azimuth and elevation axes) and the local network. This and other error sources are discussed in the following section.

17

VI. Discussion of Errors

In this section, we discuss the sources of error in the results presented in Section V. Error sources are categorized as either associated or not associated with parameters that are estimated in the least-squares sense. They are also categorized as being sources of systematic or random error. Within this framework, an error budget is developed for the specific example of the 245 km length OVRO/Mojave baseline. Tests are made of the dependence of mobile baseline accuracy on data noise, multipathing, a priori information and fiducial network GPS constellation geometry. Comparisons are then made between this error budget and the results presented in the previous section for day-to-day baseline repeatability and for GPS/VLBI baseline intercomparison.

Systematic Errors Associated With Non-Estimated Parameters

Many model parameters are not adjusted in the least-squares estimation process. These include fiducial station coordinates, earth orientation parameters, a coordinate scale factor, solar radiation parameters, and geocenter coordinates. (See Table 6 for a more complete tabulation of these.) In the case of all but the first of these parameters, estimation was not attempted, because the HPBT data lack the strength to make meaningful estimations of their values. In the case of the fiducial station coordinates, estimation is precluded by the requirement that a consistent definition of the GPS coordinate frame be maintained for all GPS geodetic results.

The contributions of uncertainties in these non-estimated parameters to the covariances of the estimated parameters of interest (i.e., mobile baseline components) are calculated using a technique known as consider analysis [e.g.,

Yunck and Wu, 1983; Bierman, 1977]. The non-estimated parameters to which this approach is applied are known as considered parameters and the resulting contributions to mobile baseline covariances are known as consider errors. The consider errors for non-estimated parameters in this work (listed in Table 6) were computed, and all, with the exception of those associated with fiducial station uncertainties, were found to be negligible, being $\leq$ 1 mm in size.

The consider errors associated with fiducial station location uncertainties are much larger than this. These were determined for all mobile baselines connecting the six receivers located at the Mojave, OVRO, Hat Creek and Mammoth Lakes sites. An a priori uncertainty of 4 cm was assumed in each coordinate for each of the four fiducial receivers, with local survey error providing the dominant contribution to this. (See Section IV.) These consider errors were found to be relatively large and to scale with baseline length. A plot of this length dependence is shown in Figure 7, with the separate contributions shown for the individual fiducial stations.

Several important features are evident in this figure. First, for the particular network of fiducial and mobile stations used in the Spring 1985 HPBT, the uncertainties in mobile baselines (all of which are located in California) are most sensitive to errors in the locations of the fiducial stations at OVRO, CA, and Ft. Davis, TX, with sensitivity to fiducial station errors at Westford, MA, and Richmond, FL, being smaller by factors of 3-4. Second, the total (three-dimensional) consider error for regional mobile baselines (of length $\leq$ 1000 km) is 8 cm, or less. From these facts one can conclude that reduction of local survey error to the level of a few millimeters, which is well within the capability of current techniques, would leave VLBI baseline error as the dominant contributor to uncertainty in

fiducial station location and reduce fiducial station consider error by a factor of almost ten to less than a centimeter even for baselines approaching 1000 km in length.

Systematic Errors Associated With Estimated Parameters

Since it is rarely the case that the phenomena of nature are modeled with perfect realism, it is necessary to ask what systematic errors might arise in the mobile baselines because of modeling errors associated with estimated parameters. Three sets of parameters deserve particular examination in this regard: those describing the spacecraft trajectories, the troposphere, and the ionosphere.

To investigate modeling errors in the case of spacecraft trajectories, a covariance analysis was performed to determine the sensitivity to errors in the gravity field, solar oblateness, the solar flux constant, the value of GM, and uncertainties in solar panel positioning [J. S. Border, personal communication, 1987]. These error sources were found to be negligible, particularly for the relatively short arcs and regional extent of the observing network of the Spring 1985 HPBT. In addition, to validate implementation of the orbital dynamics model in software, comparisons were made between trajectories generated by the JPL-developed PATH-VARY code and those generated by similar codes developed independently at the Aerospace Corporation and the Defense Mapping Agency. In these comparisons, six-parameter spacecraft epoch states were numerically integrated forward in time using all three codes. Agreement was observed in all cases at the level of 14 cm, or better, for arcs of up to 8 days in length. Based on these tests, we conclude that virtually no systematic error arises in this work from the mismodeling of spacecraft orbital dynamics.

In the case of the troposphere, the zenith delay at each station was modeled as the sum of wet and dry calibrations and an estimated additive constant delay having the scale height of the wet troposphere component. In conditions of high humidity, such as may be encountered in the tropical climates (e.g., the Caribbean and South America), the modeling error resulting from this approach may be significant, owing to the possible existence of horizontal gradients, which may be variable in both space and time [e.g., Treuhaft and Lanyi, 1987]. Further, an effective zenith error in the applied calibrations may not be well-represented by a constant, owing to both instrumental and meteorological effects. In the present work, however, especially given the relative quiescence of the troposphere in most of the United States, this representation may be adequate to assure that no substantial systematic error arises from mismodeling of the troposphere. Nevertheless, acknowledging the possible presence of these error sources, and lacking a more quantitative understanding of their significance, we have represented them in our error model by a 1 cm systematic (consider) error in the zenith dry troposphere and a 0.5 cm uncertainty in each mobile horizontal baseline component.

It warrants mention that a stochastic white noise representation of the clocks—in effect, elimination of clocks by double differencing—assures that no systematic error in the mobile baselines arises from the mismodeling of clocks. This may not generally be the case in future work, should other representations of clock behavior—such as linear, quadratic or stochastic colored noise—be used.

In the case of the ionosphere, dispersive effects are removed using an assumed inverse-squared frequency dependence, as described earlier. (See Section IV.) The size of higher-order effects on the dual frequency phase

observable was calculated for the worst-case scenario of observation during solar maximum at midday at low elevation. It was found to be less than 1 cm [S. A. Stephens, personal communication, 1986]. Since the Spring 1985 HPBT took place during the solar minimum and at night, we conclude that systematic errors due to ionosphere mismodeling are reduced by over an order of magnitude from the worst case and are negligible.

Random Errors

Those estimated parameters for which no significant modeling errors exist are removed as sources of systematic error by means of their adjustment in the least-squares estimation process. Parameters in this class include all those listed as estimated in Table 6, with the possible exception, as noted above, of those characterizing the troposphere. The impact of these parameters on computed baseline covariances (i.e., formal errors) may be significant, depending in size on a combination of factors, including observable noise, a priori information, and network geometry. However, it must be emphasized that parameters in this class are not to be regarded as sources of error, in the sense that their impact on the system performance is always appropriately reflected in the size of the computed baseline covariances. To investigate the dependence of baseline accuracy in the Spring 1985 HPBT on these factors, test runs were made as described in the following subsections.

a. The effect of observable noise

The dependence of baseline formal errors on the assumed uncertainty, or noise, ascribed to the observable data will, in the absence of a priori information and consider errors, be exactly linear. Since the analysis of the

present work involves both of these, this linearity cannot be assumed. To investigate the dependence of formal errors on data noise, a subset of the HPBT data was reprocessed using a data noise of 2.0 cm, twice that adopted in Section IV based on post-fit RMS scatter. It was found that baseline formal errors scaled linearly with input data noise to within a few percent. This means that baseline precision will benefit directly and significantly in future experiments when improvements in the field equipment, calibrations or modeling in software reduce post-fit RMS scatter and mandate the use of smaller values for the data noise.

b.   The effect of multipathing

GPS signals which reach the receiver antenna indirectly after reflection from surfaces either near the broadcasting antenna or on the ground may sum coherently (and generally out of phase) with the direct signal and cause an error in the measured values of the phase and group delay observables. This phenomenon is known as multipathing and is highly dependent on antenna design and environment.

To examine the HPBT carrier phase data for evidence of ground-based multipathing and to investigate dependence on antenna design, meteorologically and ionospherically calibrated carrier phase observables were double-differenced, with the stations and satellites chosen to maximize the length of the arc. A model observable was subtracted, and a low-order polynomial was fit to the residual. The final residual, after removal of the fitted polynomial, should exhibit only the effects of system noise, tropospheric and instrumental fluctuations, and multipathing. Of these, only multipathing will be periodic on a sidereal day. Hence, if multipath is a significant contribution to error

in the observables, data from consecutive days will be correlated. Figures 8 and 9 show these post-fit residuals and cross-correlations for the TI-4100 and SERIES-X data, respectively, from the Mojave and OVRO sites for two days of the HPBT [Stephens et al., 1986]. These figures show multipathing to be strong for the TI-4100 antennas, but relatively weak for the SERIES-X antennas. This difference is not unexpected, since the SERIES-X antennas were placed closer to the ground (Table 4) and were equipped with back-plane absorbers, both of which suppress multipathing [e.g., Counselman et al., 1981; Crow et al., 1985; Bishop et al., 1985]. Studies are currently under way at JPL to determine the optimum ground-based receiver antenna design and environment for geodetic and tracking applications using GPS signals [L. E. Young, personal communication, 1987].

To examine the filter output for evidence of ground-based multipathing, the post-fit RMS scatter was tabulated for: (a) all receivers, (b) separate receiver types, and (c) individual receivers. It was found that the RMS scatter of undifferenced, ionosphere calibrated carrier phase observables, when all receivers were included, was about 7.5 mm, substantially larger (in an RSS sense) than the values inferred from Figures 8 and 9 for the multi-pathing components alone, which were 4 mm for TI-4100 receivers and 2 mm for SERIES-X receivers [Stephens et al., 1986]. In addition, it was found that the RMS scatters for cases (b) and (c) were also about 7.5 mm, independent of which receiver was used. From this, we conclude that ground-based multipath was not the dominant component in the data residuals and was not a limitation on system precision during the HPBT for solutions using the carrier phase data type.

For analyses utilizing the pseudorange data type, the situation is much different. Pseudorange is attractive because of its greater information

content (no range biases need be estimated), its immunity to cycle slips and its high tolerance of outages [Yunck, 1985]. However, examination of post-fit residuals in analyses attempted using pseudorange indicates a ground-based multipathing component of 50 cm, or greater, for this data type [Lichten and Border, 1987]. This is not unexpected, since multipath error scales roughly with wavelength, which for pseudorange is 100 times that for carrier phase [Yunck, 1985]. However, it should be noted that pseudorange may become the data type of choice within the next few years, with the advent of advanced GPS receivers, equipped with improved antennas capable of delivering high precision ($\leq$ 10 cm) pseudorange [Meehan et al., 1987]. Indeed, covariance analysis has shown that pseudorange with measurement noise of 20 cm, or better, will provide orbit and baseline precision comparable to that obtained using carrier phase with measurement noise of 1 cm [Bertiger et al., 1986].

Multipathing from the GPS spacecraft is expected to vary slowly with time and hence be a possible source of systematic error. This phenomenon is also under current study at JPL [Young et al., 1985; R. Neilan, 1986].

    c.   The effect of a priori information

        The dependence of baseline formal errors on the a priori uncertainties, or constraints, applied to other estimated parameters may be significant. This is particularly the case when a priori and post-fit formal errors are comparable, indicating that for these parameters, and possibly for others, the filter solutions do not derive their strength from the observable data alone. An examination of post-fit uncertainties in this work shows that only in the case of the troposphere parameters is it likely that significant a priori information has been supplied. For example, the estimated zenith troposphere

corrections at Mojave and OVRO have formal errors typically in the range 1.0-1.5 cm, only slightly smaller than the adopted value of 2.0 cm, representing the combined accuracy of the wet and dry troposphere calibrations.

To investigate this dependence, the data from April 2, 1985, were processed through the filter a number of times, with a wide range of values used for the troposphere a priori uncertainty at the Mojave and OVRO stations. Figure 10 shows a plot of the formal error in the vertical baseline component for the Mojave/OVRO baseline, the component usually most sensitive to troposphere calibration errors, as a function of troposphere a priori uncertainty. For a troposphere calibration accuracy of 2.0 cm, used in this work to represent the combined uncertainty in the wet and dry tropospheres, the resulting improvement in vertical baseline precision is only 7%. Even for a total troposphere error of 1.0 cm, it would have been only 14%. From this figure, one can infer that the use of external troposphere calibration for the processing of the data from the Spring 1985 HPBT contributed little to the precision of the estimated vertical baseline components. Further, one can infer that external calibration would have contributed significantly to this precision only if it had been on the order of 0.5 cm or better.

It should be emphasized that the above conclusions relate to the Spring 1985 HPBT only and should not be extrapolated to GPS-based geodesy in general. There are several reasons for withholding from this generalization. First, WVR-based calibration is in fact expected to eventually attain an accuracy of 0.5 cm or better [Gary et al., 1985]. Further, in conditions of high humidity, such as may be encountered in the Caribbean and South America, the existence of azimuthal asymmetries in the troposphere [e.g., Treuhaft and Lanyi, 1987] may mandate the use of WVRs for calibration via satellite copointing. In addition, the improved quality of GPS data from new receivers [Meehan et al.,

26

1987] may increase the sensitivity of baseline solutions to calibration errors. Lastly, the above claim implicitly assumes the validity of the error model and disregards the fact that the WVR calibrations provide information on the time-dependence of the wet troposphere delay; important complementary information regarding troposphere-related errors will be provided by studies (in progress) of baseline repeatability as a function of calibration technique.

> d.   The effect of fiducial network geometry

The dependence of baseline formal errors on fiducial network geometry must be understood in order to plan for future experiments. In addition, it is important to be able to predict the consequences of the loss of one or more fiducial stations during an experiment, an all too possible occurrence. To investigate this dependence, a subset of the Spring 1985 HPBT data was reprocessed using hypothetical single-station outages at Ft. Davis, Richmond and Westford in different runs. The case of a hypothetical outage at two stations simultaneously, Westford and Richmond, was also investigated. Finally, the case of a five-station fiducial network (Westford, Richmond, Ft. Davis, Mojave and OVRO) was run. The resulting formal errors in the horizontal plane for the OVRO/Mammoth (70 km), OVRO/Mojave (245 km) and Mojave/Mammoth (313 km) baselines are displayed in Figures 11 and 12. From these figures, we see that while the addition of a fifth fiducial station provides only a slight improvement in baseline precision, the loss of a station, reducing the fiducial network to three stations, results in a serious loss of precision, particularly in the case of the longer two of these three baselines. By far, the most serious loss of precision occurs when the Westford station is lost to the

fiducial network. This is not surprising, since the loss of Westford would

result in the greatest reduction in geometric extent, for both the north and

the east directions, of the fiducial network. We also see that the loss of

two fiducial stations, requiring the use of a more local fiducial network

consisting of Ft. Davis, Mojave and OVRO, results in serious loss of precision

for even the short OVRO/Mammoth baseline.

We conclude that the minimal fiducial network for GPS-based regional

geodesy using the current receiver systems consists of four stations, with a

fifth station highly desirable to protect against the possibility of an outage

somewhere within the fiducial network. We must add the following caveat: this

conclusion may not apply when improved data quality (including usable pseudo-

range) and vastly different receiver networks exist, and it will have to be

reexamined from time to time as the GPS systems evolve.

   e.   The effect of GPS satellite geometry and time-tag offsets

      Baseline results in this work (e.g., Figure 4 and Table 7) show the

precision of the eastern baseline component to be worse than that for the north

by factors of 2-4. This asymmetry is related to receiver time tag errors and

the necessity of estimating carrier phase biases without accurate pseudorange

or good a priori constraints. All ground tracks of GPS satellites at mid-

latitudes run almost exactly north to south (or south to north). Because of

this, the estimates of both carrier phase bias and time tag offsets from UTC

are correlated with the estimated longitude of a given receiver relative to

some reference receiver [Blewitt, 1987a].

In future experiments, this eastern error can be reduced by a factor of

about two, if the receiver time tags are synchronized to UTC to within a

microsecond. This would permit the application of a priori time tag constraints, breaking the correlation with longitude. Alternatively, even imprecise (e.g., 1 meter) pseudorange may be used in conjunction with carrier phase to establish clock synchronization, if there is no significant ($\geq$ 1 μsec) offset between the pseudorange and carrier phase time tags. This eastern error can be reduced by an additional factor of two by "optimizing" the carrier phase biases, using the extra information that they can assume only integer values [Blewitt, 1987b].

A GPS Error Budget

In this subsection, a GPS baseline error budget is presented for the specific case of the 245 km OVRO/Mojave baseline between the SERIES-X receivers. This error budget includes the contributions from all significant error sources, including consider errors, modeling errors in estimated parameters, and formal, or random, errors, as discussed in the preceding subsections. That is, it represents our current understanding of the absolute accuracy of the JPL-developed GPS-based geodetic systems used in the Spring 1985 HPBT. This error budget is shown for the horizontal plane in Figures 13 and 14. In these figures, the separate consider errors for geocenter uncertainty, solar radiation pressure uncertainty, coordinate scale error, earth orientation errors, and fiducial coordinate errors are shown. The a priori uncertainties used for these parameters are listed in Table 6. (The consider errors for the other non-estimated parameters are even smaller than those shown in the two figures.)

A 0.5 cm uncertainty representing the possible existence of horizontal gradients in the troposphere (i.e., modeling error) [Davidson and Trask, 1985] and the formal errors are also shown.

In examining these figures, we see that three error sources dominate all others: the fiducial station consider errors, troposphere modeling errors and formal errors. Further, we see that for the northern baseline component, no one of these three dominates, although the formal error is the smallest; for the eastern baseline component, the formal error is the largest. The total absolute accuracy inferred for the Spring 1985 HPBT results from the aggregate of all contributions is about 1.6 cm in the north and 2.6 cm in the east, or $6:10^8$ and $1:10^7$, respectively.

In the next subsections, we compare this error budget with the experimental results from this work for day-to-day repeatability of GPS measurement and with the results for colocated GPS and VLBI measurement.

Comparison of the Error Budget with Baseline Repeatability

Before comparing the results for day-to-day repeatability (Section V and Table 7) with the error budget presented in the preceding subsection, we must first recognize that not all of the error sources which contribute to the total absolute uncertainty will diminish the ability of the GPS-based systems to make reproducible measurements on short time scales. Indeed, we note that the only error source which is likely to have affected repeatability for the HPBT is the formal, or random, error.

Fiducial coordinate consider errors will not affect repeatability, because they will, to the extent that an identical observing schedule was followed on all days, be common to all days of the HPBT. Since the schedules were nominally identical on all days, differing slightly in practice only because of occasional outages within the network, we can dismiss fiducial coordinate errors as having contributed significantly to degradation of day-to-day repeatability. Similar arguments may be made in the case of troposphere modeling

30

errors, especially in view of the relatively small wet troposphere delays at the North American sites. However, this claim is made with less confidence than in the case of the fiducial sites, because the character of unmodeled horizontal gradients may sometimes change on a time scale of less than the six-day span of the HPBT.

Accepting these assumptions, we predict from our error budget an RMS repeatability of about 0.4 cm in the north and 2.4 cm in the east for the Mojave/OVRO baseline between SERIES-X receivers. From the earlier summaries given in Section V and Table 7, we have, for the HPBT data, observed values of 0.6 cm and 2.5 cm, respectively. This is in excellent agreement with the prediction of the error budget, although the small sample size (4 measurements) leaves open the possibility that this agreement is somewhat specious.

Comparison of the Error Budget with GPS/VLBI Differences

Before comparing GPS/VLBI baseline differences with the predictions of the GPS error budget, we must first recognize that there is an additional error source that contributes to the total uncertainty in the comparison (but not to the uncertainty in either the GPS or VLBI result alone). This is the 4 cm uncertainty (see Section IV) in the local (length $\leq$ 1 km) site survey measurements which must be used at the mobile GPS sites to relate the VLBI- and GPS-based measurements. Thus, the total uncertainty for either component in this comparison is given by the summation in quadrature of this 4 cm survey error and the total (RSS) uncertainty shown in Figure 13 or 14.

From this, we obtain an uncertainty (one standard deviation) in the difference of the GPS and VLBI measurements of 4.3 cm in the north and 4.8 cm in the east for the Mojave/OVRO baseline between SERIES-X receivers. Consulting the earlier summaries given in Section V and Table 7, we have, from the

HPBT experimental results, mean values of 2.1 cm and 5.6 cm, respectively, for this baseline, in agreement with the predictions of our error budget. Similar conclusions apply to the other GPS/VLBI comparisons made in Figure 6.

It should be noted that the uncertainty in these GPS/VLBI intercomparisons is dominated by the hypothesized 4 cm error in the local survey measurement. If this survey error is reduced to the level of a few millimeters, which is certainly within the capability of current techniques, then the uncertainty in the VLBI/ GPS intercomparison will decrease substantially, to about 1.8 cm (north) and 2.6 cm (east) for the above example of the Mojave/OVRO SERIES-X baseline, enabling a much more stringent test of the accuracy of the GPS-based geodetic systems. Because of this fact, new local surveys of the Mojave and OVRO sites using mobile VLBI measurement are planned for the Fall of 1987. Similar resurveys of the POLARIS VLBI sites are being considered [R. J. Coates and J. W. Ryan, personal communication, 1987].

VII. Summary and Conclusion

In this report, we have presented a description of the Spring 1985 High Precision Baseline Test (HPBT), in which a collaborative effort was mounted under the leadership of the Jet Propulsion Laboratory to conduct a measurement campaign involving over a dozen institutions and having fourteen GPS-based geodetic systems deployed to ten sites across the United States. In analysis of the HPBT data, it was demonstrated that system performance was at a level of $1-2:10^7$ for baselines approaching 1000 km in length, thus meeting the accuracy objectives of the test. System precision was shown to be better than this for some baseline components by a factor of 2-4. Although this level of

accuracy meets the minimum criterion for usefulness in a program of scientific research, it falls short by an order of magnitude, or more, of the performance level of current VLBI-based systems. However, insights gained in the course of analyzing the HPBT data confirm the expectation that GPS-based geodesy will eventually rival the accuracy of VLBI systems. Several specific improvements required in the GPS system to reach this accuracy goal have been cited in the preceding text. We summarize them here briefly.

a. Improved fiducial site surveys are required to reduce fiducial baseline uncertainty to $\leq$ 1 cm.

b. Improved troposphere calibration data must be taken, particularly in regions of high humidity. This will require more and improved WVRs, capable of GPS satellite copointing, and improved and standardized surface meteorology sensors.

c. Improved antenna design and environmental control are required to reduce multipathing for pseudorange observables to a few centimeters.

d. Improved receivers are required which can view all visible satellites, eliminate cycle slips in carrier phase data, synchronize time tags to within 1 μsec of UTC for both carrier phase and pseudorange, and deliver precision ($\leq$ 10 cm) pseudorange.

e. Improved analytical techniques are required which will fully exploit the above improvements. These include: the use of data from multiple days in estimating ephemerides; the use of statistical, or stochastic, models as more representative of clock, troposphere and (possibly) ionosphere behavior; and the use of bias optimization to

incorporate the discrete character of the range biases into the estimation of baselines.

f.   Although it is not in our power to affect the GPS constellation itself, we note that, using the most recent launch schedule, the current GPS constellation of six Block I satellites will have been replaced by twenty-four Block II satellites by the end of 1992. This will not only improve observing geometry (given the implementation of item (d) above), but it will also permit experiments to be conducted at any hour of the day. (Presumably, they will always be done at night, when the troposphere and ionosphere are more stable and the effect of the ionosphere is minimal.)

Covariance analysis, combined with our experience with new data collected since the HPBT, indicates that when the above improvements have been implemented, GPS-based geodetic systems will rival the VLBI-based systems in accuracy, while being an order of magnitude less expensive to both obtain and operate. This will open the door to the participation in geodetic measurement programs by many organizations for which VLBI-based geodesy is now too costly. That participation in turn will lead to increased resolution in the measurement of regional strain fields and intercontinental crustal motion, leading ultimately to more stringent tests of models of tectonic plate driving forces and to an improved understanding of the interior structure of the Earth.

VIII. References

Bertiger, W. I., S. C. Wu, J. S. Border, S. M. Lichten, B. G. Williams and
T. J. Wu, High precision GPS orbit determination using March 1985 demonstration data, AIAA 24th Aerospace Sciences Meeting, paper AIAA-86-0089, Reno, NV, January 1986.

Bierman, G. J., Factorization methods for discrete sequential estimation, 241 pp., Academic Press, New York, NY, 1977.

Bishop, G. J., J. A. Klobuchar and P. H. Doherty, Multipath effects of the determination of absolute ionospheric time delay from GPS signals, Radio Sci., 20, 388-396, 1985.

Blewitt, G., On improving the estimation of relative longitude in GPS-based systems, JPL Interoffice Memorandum 335.1-87-41 (internal document), Jet Propulsion Laboratory, Pasadena, CA, May 1987.

Blewitt, G., The expectation value approach to optimization of range biases in carrier phase observables (abstract), Eos Trans. AGU, 68, 285, 1987.

Bock, Y., R. I. Abbot, C. C. Counselman III, S. A. Gourevitch, and R. W. King, Establishment of three-dimensional geodetic control by interferometry with the Global Positioning System, J. Geophys. Res., 90, 7689-7703, 1985.

Chao, C. C., A new method to predict wet zenith range correction from surface measurements, JPL Technical Report 32-1526, 14, pp. 33-41, Jet Propulsion Laboratory, Pasadena, CA, 1973.

Christodoulidis, D. C., D. E. Smith, R. Kolenkiewicz, S. M. Klosko, M. H. Torrence, and P. G. Dunn, Observing tectonic plate motions and deformations from satellite laser ranging, J. Geophys. Res., 90, 9249-9264, 1985.

Counselman, C.C., III, and S. A. Gourevitch, Miniature interferometer terminals for earth surveying: ambiguity and multipath with global positioning system, IEEE Trans. Geosci. Remote Sens., GE-19, 244-252, 1981.

Crow, R. B., F. R. Bletzacker, R. J. Najarian, G. H. Purcell, Jr., J. I. Statman, and J. B. Thomas, SERIES-X final engineering report, JPL Internal Document D-1476, Jet Propulsion Laboratory, Pasadena, CA, August 1984.

Davidson, J. M. and D. W. Trask, Utilization of mobile VLBI for geodetic measurements, IEEE Trans. Geosci. Remote Sens., GE-23, 426-437, 1985.

Davidson, J. M., C. L. Thornton, T. H. Dixon, C. J. Vegos, L. E. Young, and T. P. Yunck, The March 1985 demonstration of the fiducial network concept: a preliminary report, in Proceedings of the First International Symposium on Precise Positioning with the Global Positioning System, edited by C. Goad, pp. 603-612, NOAA, Rockville, MD, 1985; and TDA Progress Report 42-85, pp. 212-218, Jet Propulsion Laboratory, Pasadena, CA, 1986.

Gary, B. L., S. J. Keihm and M. A. Janssen, Optimum strategies and performance for the remote sensing of path-delay using ground-based microwave radiometers, IEEE Trans. Geosci. Remote Sens., GE-23, 479-484, 1985.

Hensen, D. J., E. A. Collier and K. R. Schneider, Geodetic applications of the Texas Instruments TI-4100 GPS navigator, Proceedings of the First International Symposium on Precise Positioning with the Global Positioning System, edited by C. Goad, pp. 191-200, NOAA, Rockville, MD, 1985.

Herring, T. A., I. I. Shapiro, T. A. Clark, C. Ma, J. W. Ryan, B. R. Schupler, C. A. Knight, G. Lundqvist, D. B. Shaffer, N. R. Vandenberg, B. E. Corey, H. F. Hinteregger, A. E. E. Rogers, J. C. Weber, A. R. Whitney, G. Elgered, B. O. Ronnang, and J. L. Davis, Geodesy by radio interferometry: evidence for contemporary plate motion, J. Geophys. Res., 91, 8341-8347, 1986.

Hothem, L. D., T. Vincenty, and R. E. Moose, Relationship between doppler and other advanced geodetic system measurements based on global data, in _Proceedings of the Third International Geodetic Symposium on Satellite Doppler Positioning_, New Mexico State University, NM, February 1982.

Kroger, P. M., G. A. Lyzenga, K. S. Wallace, and J. M. Davidson, Tectonic motion in the western United States inferred from very long baseline interferometry measurements, 1980-1986, submitted to _J. Geophys. Res._, March 1987.

Ladd, J. W., and C. C. Counselman III, The Macrometer II™ dual-band interferometric surveyor, in _Proceedings of the First International Symposium on Precise Positioning with the Global Positioning System_, edited by C. Goad, pp. 175-180, NOAA, Rockville, MD, 1985.

Lanyi, G., Tropospheric calibration in radio interferometry, in _Proceedings of the International Symposium on Space Techniques for Geodynamics_, edited by J. Somogyi and Ch. Reigber, pp. 184-195, IAG/COSPAR, Sopron, Hungary, July 9-13, 1984.

Lichten, S. M., J. S. Border, S.-C. Wu, B. G. Williams, and T. P. Yunck, Precise GPS orbit determination results from 1985 field tests, paper presented at AIAA/AAS Astrodynamics Conference, Williamsburg, VA, August 18-20, 1986.

Lichten, S. M., and J. S. Border, Strategies for high precision GPS orbit determination, submitted to _J. Geophys. Res._, June 1987.

Meehan, T. K., J. M. Srinivasan, J. B. Thomas, T. N. Munson, R. E. Neilan and L. E. Young, Baseline tests of the JPL ROGUE receiver (abstract), _Proceedings of the General Assembly, International Union of Geodesy and Geophysics_, Vancouver, B.C., Canada, 1987.

Melbourne, W. G., J. M. Davidson, T. H. Dixon, M. P. Golombek, C. L. Thornton and C. J. Vegos, GPS measurement system development for regional geodesy: operating plan, JPL Internal Document D-3562, Jet Propulsion Laboratory, Pasadena, CA, August 1986.

Minster, J. B., and T. H. Jordan, Present-day plate motions, J. Geophys. Res., 83, 5331-5354, 1978.

Moyer, T. D., Mathematical formulation of the double-precision orbit determination program (DPODP), JPL Technical Report 32-1527, Jet Propulsion Laboratory, Pasadena, CA, May 1971.

NASA, Crustal Dynamics Project catalogue of site information, NASA/GSFC Technical Report X-904-83-14, Goddard Space Flight Center, Greenbelt, MD, September 1983.

Neilan, R. E., An experimental investigation of the effect of GPS satellite multipath, ROMI M. S. Thesis, University of Wisconsin, Madison, WI, 1986.

Robinson, S. E., A new algorithm for microwave delay estimation from water vapor radiometer data, TDA Progress Report 42-87, pp. 149-157, Jet Propulsion Laboratory, Pasadena, CA, 1986.

Rundle, J. B., and J. H. Whitcomb, A model for deformation in Long Valley, California, 1980-1983, J. Geophys. Res., 89, 9371-9380, 1984.

Ryan, J. W., and C. Ma, Crustal Dynamics Project data analysis: fixed station VLBI geodetic results, NASA/GSFC Technical Memorandum 86229, Goddard Space Flight Center, Greenbelt, MD, October 1985.

Savage, J. C., and M. M. Clark, Magmatic resurgence in Long Valley caldera, California: possible cause of the 1980 Mammoth Lakes earthquakes, Science, 217, 531-533, 1982.

Sims, M. L., Phase center variation in the geodetic TI 4100 receiver system's conical spiral antenna, in <u>Proceedings of the First International Symposium on Precise Positioning with the Global Positioning System</u>, edited by C. Goad, pp. 227-244, NOAA, Rockville, MD, 1985.

Smith, D. E., D. C. Christodoulidis, R. Kolenkiewicz, P. J. Dunn, S. M. Klosko, M. H. Torrence, S. Fricke and S. Blackwell, A global geodetic reference frame from LAGEOS ranging, <u>J. Geophys. Res.</u>, <u>90</u>, 9221-9234, 1985.

Sovers, O. J., and J. S. Border, Observation model and parameter partials for the JPL geodetic GPS modeling software "GPSOMC," JPL Publication 87-21, Jet Propulsion Laboratory, Pasadena, CA, August 1987.

Sovers, O. J., and J. L. Fanselow, Observation model and parameter partials for the JPL VLBI parameter estimation software "MASTERFIT"-1986, JPL Publication 83-39, Rev. 2, Jet Propulsion Laboratory, Pasadena, CA, August 1986.

Sovers, O. J., J. B. Thomas, J. L. Fanselow, E. J. Cohen, G. H. Purcell, Jr., D. H. Rogstad, L. J. Skjerve and D. L. Spitzmesser, Radio interferometric determination of intercontinental baselines and earth orientation utilizing Deep Space Network antennas: 1971 to 1980, <u>J. Geophys. Res.</u>, <u>89</u>, 7597-7607, 1984.

Stephens, S. A., J. M. Davidson, C. L. Thornton and G. Blewitt, GPS receiver performance intercomparisons from the 1985 Spring and Fall High Precision Baseline Tests (abstract), <u>Eos Trans. AGU</u>, <u>67</u>, 262, 1986.

Tapley, B. D., B. E. Schutz and R. J. Eanes, Station coordinates, baselines and Earth rotation from LAGEOS laser ranging, <u>J. Geophys. Res.</u>, <u>90</u>, 9235-9248, 1985.

Treuhaft, R. N., and G. E. Lanyi, The effect of the dynamic wet troposphere on radio interferometric measurements, <u>Radio Sci.</u>, <u>22</u>, 251-265, 1987.

Wu, S.-C., W. I. Bertiger, J. S. Border, S. M. Lichten, R. F. Sunseri, B. G. Williams, P. J. Wolff, and J. T. Wu, OASIS mathematical description, V 1.0, JPL Internal Document D-3139, Jet Propulsion Laboratory, Pasadena, CA, 1986.

Wu, S.-C., and C. L. Thornton, OASIS--a new GPS covariance and simulation analysis software system, in Proceedings of the First International Symposium on Precise Positioning System, edited by C. Goad, pp. 337-346, NOAA, Rockville, MD, 1985.

Young, L. E., R. E. Neilan and F. R. Bletzacker, GPS satellite multipath: an experimental investigation, in Proceedings of the First International Symposium on Precise Positioning with the Global Positioning System, edited by C. Goad, pp. 423-432, NOAA, Rockville, MD, 1985.

Yunck, T. P., Multipath and the geodetic use of P code, JPL Interoffice Memorandum 335.1-331 (internal document), Jet Propulsion Laboratory, Pasadena, CA, August 1985.

Yunck, T. P., and S.-C. Wu, Tracking geosynchronous satellites by very-long-baseline interferometry, J. Guidance, Control, and Dynamics, 6, 382-386, 1983.

Table 1. Spring 1985 HPBT Participating Institutions and Organizations

---

NASA Geodynamics Program

Applied Research Laboratory

Air Force Geophysical Laboratory

Bendix Corporation

California Institute of Technology

Crustal Dynamics Project

Defense Mapping Agency

Haystack Observatory

Interferometrics Incorporated

Jet Propulsion Laboratory

National Geodetic Survey

Naval Surface Weapons Center

Pacific Missile Test Center

Texas Department of Highways

Texas Instruments Corporation

United States Geological Survey

University Navstar Consortium

Table 2. Summary of Field Equipment Information

Station	Receiver[a]	WVR[a]	Frequency Standard
Austin, TX	ARL TI-4100		Quartz
Dahlgren, VA	ARL TI-4100		Quartz
Ft. Davis, TX	TDH TI-4100		H-Maser
	AFGL dual-frequency		H-Maser
Hat Creek, CA	TI-4100	DSN Prototype	Various[b]
Mammoth Lakes, CA	ARL TI-4100		Quartz/Rb[c]
Mojave, CA	JPL SERIES-X	CDP J01	H-Maser
	TI TI-4100		Various[b]
OVRO, CA	JPL SERIES-X	CDP Prototype	H-Maser
	TI TI-4100		Various[b]
Pt. Mugu, CA	PMTC TI-4100		Quartz
Richmond, FL	ARL TI-4100		H-Maser
	AFGL dual-frequency		H-Maser
Westford, MA	ARL TI-4100		Quartz
	AFGL dual-frequency		H-Maser

[a] Institutional cognizance of GPS receivers and WVRs used in the HPBT
is denoted by the first set of initials in these two columns. The meanings of
those abbreviations are as follows: AFGL, Air Force Geophysical Laboratory;
ARL, Applied Research Laboratory; CDP, NASA Crustal Dynamics Project; DSN,
NASA Deep Space Network; JPL, Jet Propulsion Laboratory; PMTC, Pacific Missile
Testing Center; TDH, Texas Department of Highways; TI, Texas Instruments Cor-
poration. The different WVR types are as follows. The prototype WVRs were
developed at JPL for the CDP in 1980-1984. The retrofit WVRs are prototype

models which have been upgraded by the Bendix Corporation under contract to the CDP. The J01 WVR is a new prototype developed at JPL for the CDP in 1984-1985.

[b] These receivers were operated using Rb clocks on March 31 and April 1; quartz oscillators on April 2, 3, and 5; and hydrogen masers on April 4, with the objective of investigating the dependence of baseline accuracy on the frequency standard.

[c] This receiver was operated using a Rb clock on March 31, April 1 and April 4, and quartz oscillators on April 2, 3, and 5. No hydrogen maser was available at this site.

Table 3. A Priori Geocentric Station Monument Coordinates

Station	Receiver	x (meters)	y (meters)	z (meters)
Ft. Davis	AFGL,TI-4100	-1324191.759 $\pm$0.003	-5332059.538 $\pm$0.008	3232043.630 $\pm$0.009
Hat Creek	TI-4100	-2523871.799 $\pm$0.005	-4123579.617 $\pm$0.012	4147719.343 $\pm$0.014
Mammoth Lakes	TI-4100	-2444431.955 $\pm$0.200	-4428702.740 $\pm$0.200	3875726.757 $\pm$0.200
Mojave	SERIES-X	-2356424.353 $\pm$0.004	-4646613.350 $\pm$0.010	3668462.501 $\pm$0.012
Mojave	TI-4100	-2356563.990 $\pm$0.004	-4646571.275 $\pm$0.010	3668427.653 $\pm$0.012
Owens Valley	SERIES-X	-2410422.303 $\pm$0.004	-4477802.368 $\pm$0.009	3838686.995 $\pm$0.011
Owens Valley	TI-4100	-2409643.017 $\pm$0.004	-4478268.259 $\pm$0.009	3838638.733 $\pm$0.011
Richmond	AFGL,TI-4100	961317.840 $\pm$0.005	-5674054.593 $\pm$0.013	2740563.869 $\pm$0.010
Westford	AFGL,TI-4100	1492410.115 $\pm$0.003	-4457289.988 $\pm$0.004	4296819.266 $\pm$0.004

All coordinates displayed in this table, except those for Mammoth Lakes, are based on global VLBI
solution S284C of Ryan and Ma [1985]; the survey information contained in the Crustal Dynamics Project
Catalogue of Site Information [NASA, 1983]; and a correction to the geocenter provided by R. W. King
[personal communication, 1986]. The uncertainties are taken directly from Ryan and Ma [1985] and have
not been augmented to account for possible systematic errors. The coordinates for Mammoth Lakes are
based on GPS data from the Spring 1985 ⊞PBT and do not reflect our best solution.

Table 4. Offsets of Antenna Phase Centers from Station Reference Monuments

Station	Receiver	East (meters)	North (meters)	Vertical (meters)
Ft. Davis	AFGL	-39.150	-61.521	3.412
Ft. Davis	TI-4100	0.000	0.000	1.096
Hat Creek	TI-4100	0.000	0.000	0.346
Mammoth Lakes	TI-4100	0.000	0.000	...[a]
Mojave	SERIES-X	0.000	-0.625	0.778
Mojave	TI-4100	0.000	0.000	1.744
Owens Valley	SERIES-X	0.005	-0.625	0.906
Owens Valley	TI-4100	0.000	0.000	1.749
Richmond	AFGL	-11.772	-30.567	6.569
Richmond	TI-4100	0.000	0.000	2.764
Westford	AFGL	3.470	-45.131	0.742
Westford	TI-4100	-0.003	-0.017	2.804

The offsets given reference the effective phase centers for the dual-frequency observable. The sign sense of these offsets is antenna-monument= offset.

[a] The TI-4100 antenna at Mammoth Lakes was stowed and redeployed each day. The vertical offsets in meters for the separate days were as follows for March 31, 1985, through April 5, 1985, respectively: 1.892, 1.797, 1.803, 1.800, 1.803, and 1.826.

Table 5. Station Monument Identifications

Station	Receiver	Site Number	Monument Inscription	Monument Number
Ft. Davis[a]	AFGL,TI-4100	7216	HARVARD RM 4 1980	...
Hat Creek	TI-4100	7218	LM No. 1 M	...
Mammoth Lakes	TI-4100	...	Dept. Interior, Center for Earthquake Research	... ...
Mojave	SERIES-X	7222	MOJAVE NCMN NO. 1 1983	...
Mojave	TI-4100	7222	MOJAVE NCMN NO. 3 1983	...
Owens Valley	SERIES-X	7207	MOBLAS 7114 1979	7114
Owens Valley	TI-4100	7207	BP ARIES 3	...
Richmond[a]	AFGL,TI-4100	7219	TIMER 1962	...
Westford[a]	AFGL,TI-4100	7209	OCP 3	...

All data displayed in this table are taken from the Crustal Dynamics Project Catalogue of Site Information [NASA, 1983], except for that relating to the Mammoth Lakes site, for which the monument was established in the field during the HPBT by the U.S. Geological Survey.

[a] The AFGL and TI-4100 receivers at Ft. Davis, Richmond and Westford were referenced to the same monument.

Table 6. Estimated and Considered Parameters

Parameter	Treatment	A Priori Uncertainty	Comment
Satellite Coordinates at Epoch	Estimated	20 km	
Satellite Velocities at Epoch	Estimated	1 km/sec	
Zenith Wet Tropospheres	Estimated	2.0 cm	Mojave, OVRO WVRs
		6.0 cm	Elsewhere
Mobile Station Coordinates	Estimated	2 km	
Station and Spacecraft Clocks[a]	Estimated	1 sec	Stochastic, white noise
Range Biases	Estimated	10.0 sec x c	c = speed of light
Fiducial Station Coordinates[b]	Considered[c]	4 cm	
Mobile Site Survey[b]	Considered	4 cm	Link VLBI, GPS antennas
Zenith Dry Tropospheres	Considered	1 cm	
Geocenter Coordinates	Considered	10 cm	
UT1 – UTC	Considered	0.1 msec	
x-Pole	Considered	2 mas	
y-Pole	Considered	2 mas	
Solar Radiation Parameters	Considered	5%	Reflectance[d]
		0.5×10^{-13} km/sec^2	Acceleration[e]
Reference Clock	Considered	1 μsec	
Coordinate Scale	Considered	1.4×10^{-8}	

47

^{a}A single clock must be fixed to define an absolute time reference. For most cases, this was the

OVRO SERIES-X clock.

^{b}Fiducial and mobile station a priori uncertainties include contributions from VLBI baseline error,

local site survey error and GPS antenna phase variation error.

^{c}See Section VI for a discussion of considered parameters.

^{d}Two reflectance parameters per satellite are used to model forces lying in the plane of the

spacecraft, Earth and Sun.

^{e}One acceleration parameter per satellite is used to model forces normal to the plane of the

spacecraft, Earth and Sun.

Table 7. Baseline Results from the Spring 1985 HPBT

Baseline[a]:   OVRO(SX)/MOJAVE(SX) 245 km

Date	East	North	Vertical	Length
90	5.3 (2.2) (2.7)	5.8 (0.4) (1.3)	-4.2 (1.8) (3.3)	-2.4 (1.1) (2.0)
92	-0.5 (1.7) (2.3)	4.8 (0.3) (1.3)	-4.8 (2.1) (2.6)	-4.5 (0.9) (1.9)
93	2.4 (1.6) (2.2)	6.0 (0.3) (1.4)	-9.3 (1.4) (3.4)	-4.1 (0.8) (1.9)
94	3.4 (2.8) (3.2)	6.0 (0.9) (1.0)	-1.8 (1.9) (3.5)	-3.5 (1.6) (1.9)
Mean[b]	2.1 (1.4) (6.7)	5.6 (0.4) (7.0)	-5.7 (2.0) (6.7)	-3.9 (0.5) (7.4)
RMS[c]	2.5	0.6	3.4	0.9
χ^2/d.f.[d]	1.6	2.4	3.8	0.8

Baseline[a]:   OVRO(SX)/MOJAVE(TI) 245 km

Date	East	North	Vertical	Length
90	-0.1 (2.4) (2.8)	5.9 (0.6) (1.5)	-5.7 (2.4) (3.1)	-5.3 (1.4) (2.2)
92	5.0 (2.1) (2.4)	4.9 (0.4) (1.3)	-4.1 (2.1) (2.8)	-1.8 (1.0) (1.8)
93	7.4 (2.0) (2.4)	6.6 (0.4) (1.3)	-7.4 (1.6) (3.0)	-2.0 (0.9) (1.8)
94	9.4 (2.7) (3.1)	6.6 (0.9) (1.0)	-0.1 (2.0) (3.3)	-0.9 (1.5) (1.8)
95	7.6 (3.6) (3.9)	3.7 (1.1) (1.9)	-2.9 (2.6) (3.3)	0.6 (1.3) (2.3)
Mean[b]	5.6 (1.8) (6.8)	5.7 (0.5) (7.0)	-4.4 (1.5) (6.6)	-1.8 (0.9) (7.4)
RMS[c]	3.6	1.0	3.1	1.8
χ^2/d.f.[d]	2.2	3.0	2.2	2.6

Table 7. Baseline Results from the Spring 1985 HPBT (Continued)

Baseline[a]: OVRO(TI)/MOJAVE(SX) 245 km

Date	East	North	Vertical	Length
90	10.0 (2.3) (2.7)	6.6 (0.5) (1.4)	-2.7 (1.2) (3.5)	-0.4 (1.1) (1.9)
91	2.9 (3.0) (3.3)	4.3 (0.7) (1.5)	-19.9 (1.9) (3.2)	-1.7 (1.2) (2.0)
92	-2.3 (2.2) (2.6)	5.3 (0.5) (1.3)	-15.3 (2.7) (2.9)	-5.5 (1.2) (1.9)
93	3.6 (2.1) (2.4)	6.3 (0.5) (1.4)	-10.5 (1.7) (3.4)	-3.3 (1.0) (1.8)
94	4.2 (2.8) (3.2)	6.4 (0.9) (1.0)	-1.8 (2.0) (3.3)	-3.3 (1.6) (1.9)
Mean[b]	3.6 (2.3) (7.0)	5.9 (0.4) (7.0)	-8.1 (3.8) (7.5)	-2.8 (1.0) (7.4)
RMS[c]	4.7	0.9	7.6	1.9
χ^2/d.f.[d]	3.7	2.3	20.1	2.6

Baseline[a]: OVRO(TI)/MOJAVE(TI) 245 km

Date	East	North	Vertical	Length
90	4.7 (2.4) (2.7)	6.4 (0.6) (1.5)	-4.2 (2.5) (2.8)	-3.3 (1.3) (2.0)
91	4.7 (1.8) (2.2)	6.9 (0.4) (1.4)	-15.7 (1.8) (2.7)	-3.9 (0.8) (1.7)
92	3.6 (2.2) (2.4)	4.9 (0.5) (1.3)	-14.8 (2.5) (2.7)	-2.7 (1.1) (1.7)
93	8.9 (1.9) (2.1)	6.4 (0.5) (1.4)	-8.8 (1.8) (3.0)	-1.2 (0.8) (1.6)
94	10.4 (2.6) (3.1)	6.8 (0.9) (1.0)	-0.2 (2.1) (3.0)	-0.7 (1.4) (1.7)
95	8.4 (3.5) (3.9)	4.3 (1.1) (1.9)	-1.9 (2.7) (3.3)	0.5 (1.2) (2.4)
Mean[b]	6.4 (1.2) (6.7)	6.2 (0.4) (7.0)	-8.4 (2.9) (7.1)	-2.1 (0.7) (7.4)
RMS[c]	2.7	0.9	6.6	1.6·
χ^2/d.f.[d]	1.5	2.4	9.4	2.5

Table 7. Baseline Results from the Spring 1985 HPBT (Continued)

Baseline[a]: OVRO(SX)/HAT CREEK(TI) 484 km

Date	East	North	Vertical	Length
90	1.7 (3.0) (3.8)	0.0 (0.6) (2.9)	12.1 (2.9) (3.5)	−0.5 (1.7) (3.6)
92	8.7 (3.1) (3.5)	3.1 (0.8) (3.0)	16.2 (3.0) (3.5)	−1.9 (1.6) (3.3)
93	9.4 (2.7) (3.3)	1.4 (0.7) (3.0)	9.2 (2.3) (4.0)	−4.0 (1.4) (3.2)
94	23.1 (5.2) (6.0)	5.0 (1.9) (2.1)	2.6 (3.5) (4.9)	−9.3 (3.0) (3.7)
95	12.9 (5.1) (5.7)	6.7 (2.0) (4.4)	9.5 (3.6) (4.8)	−1.7 (2.0) (4.6)
Mean[b]	8.7 (3.2) (7.3)	1.7 (1.0) (7.1)	10.3 (2.3) (6.8)	−2.7 (1.2) (7.4)
RMS[c]	6.4	2.0	4.5	2.5
χ^2/d.f.[d]	3.5	5.2	2.4	1.9

Baseline[a]: OVRO(TI)/HAT CREEK(TI) 484 km

Date	East	North	Vertical	Length
90	6.0 (2.6) (3.6)	1.2 (0.6) (2.9)	13.6 (2.5) (3.2)	−2.9 (1.4) (3.6)
91	5.8 (2.4) (3.4)	0.5 (0.6) (2.7)	5.1 (2.7) (3.1)	−3.0 (1.3) (3.4)
92	6.5 (2.8) (3.4)	4.2 (0.8) (3.1)	5.6 (2.9) (3.4)	−0.3 (1.5) (3.4)
93	10.5 (2.3) (3.1)	1.6 (0.7) (3.0)	8.1 (2.4) (3.0)	−4.8 (1.1) (3.2)
94	24.0 (5.1) (5.9)	4.6 (1.8) (2.1)	3.1 (3.5) (4.0)	−9.6 (3.0) (3.6)
95	13.5 (5.1) (5.6)	7.5 (1.7) (4.3)	10.7 (3.6) (4.2)	−1.7 (1.8) (4.5)
Mean[b]	8.6 (2.2) (6.9)	1.9 (0.8) (7.1)	8.0 (1.7) (6.6)	−3.2 (1.0) (7.4)
RMS[c]	4.8	1.8	3.8	2.2
χ^2/d.f.[d]	2.8	5.5	1.8	2.3

Table 7. Baseline Results from the Spring 1985 HPBT (Continued)

Baseline[a]: MOJAVE(SX)/HAT CREEK(TI) 729 km

Date	East	North	Vertical	Length
90	-4.4 (3.6) (5.2)	-4.8 (0.8) (4.3)	16.4 (2.8) (4.6)	-2.6 (1.9) (5.2)
91	2.3 (3.8) (5.3)	-3.0 (1.0) (4.2)	25.2 (3.0) (4.6)	-5.2 (1.7) (5.1)
92	8.4 (3.4) (4.6)	-0.6 (0.9) (4.3)	21.2 (3.0) (4.1)	-6.1 (1.7) (4.9)
93	6.5 (3.1) (4.4)	-4.2 (0.9) (4.4)	18.9 (2.5) (4.4)	-8.0 (1.6) (4.8)
94	19.8 (7.2) (8.6)	-1.9 (2.5) (3.0)	5.4 (4.6) (5.5)	-12.4 (4.3) (5.3)
Mean[b]	4.5 (3.3) (7.3)	-3.2 (0.9) (7.1)	18.9 (2.9) (7.0)	-6.0 (1.3) (7.4)
RMS[c]	6.6	1.8	5.7	2.6
χ^2/d.f.[d]	3.2	3.4	3.6	1.8

Baseline[a]: MOJAVE(TI)/HAT CREEK(TI) 729 km

Date	East	North	Vertical	Length
90	1.0 (3.7) (5.2)	-4.9 (0.9) (4.4)	17.8 (3.4) (4.3)	-5.7 (2.0) (5.3)
91	1.0 (3.1) (4.8)	-6.3 (0.8) (4.0)	20.9 (2.9) (4.4)	-7.0 (1.6) (5.0)
92	2.9 (3.2) (4.3)	-0.6 (0.9) (4.3)	20.5 (2.9) (3.9)	-3.2 (1.6) (4.7)
93	1.5 (3.0) (4.1)	-4.7 (0.9) (4.3)	17.0 (2.6) (4.1)	-5.7 (1.4) (4.6)
94	13.7 (7.1) (8.5)	-2.5 (2.6) (3.0)	3.7 (4.6) (5.7)	-9.6 (4.1) (5.2)
95	4.9 (6.3) (7.3)	3.3 (2.1) (5.8)	12.6 (4.1) (5.1)	-0.5 (2.3) (6.5)
Mean[b]	2.3 (1.3) (6.7)	-3.9 (1.2) (7.1)	17.1 (2.3) (6.8)	-5.0 (1.1) (7.4)
RMS[c]	3.0	2.8	5.2	2.4
χ^2/d.f.[d]	0.6	7.0	2.6	1.7

Table 7. Baseline Results from the Spring 1985 HPBT (Continued)

This table gives offsets of solutions from VLBI-based values.

The "baseline result" is the leftmost of the three numbers in each column. The other two numbers, in parentheses, denote the formal standard error and the total absolute error, respectively. These differ in that the latter includes contributions from systematic error sources. All values are in centimeters, except for χ^2/d.f., which is dimensionless.

[a] Receiver types are denoted by SX (SERIES-X) or TI (TI-4100). The sign sense for coordinates of the baseline Station A/Station B is Baseline = A - B, where A and B are the respective station vectors.

[b] This is a weighted mean, with weights given by the inverse squares of the formal standard errors. The formal standard error of the mean = RMS/$\sqrt{N-1}$.

[c] The weighted RMS is computed with respect to the weighted mean and does not account for error in the mean.

[d] χ^2 per degree of freedom is calculated using formal standard errors.
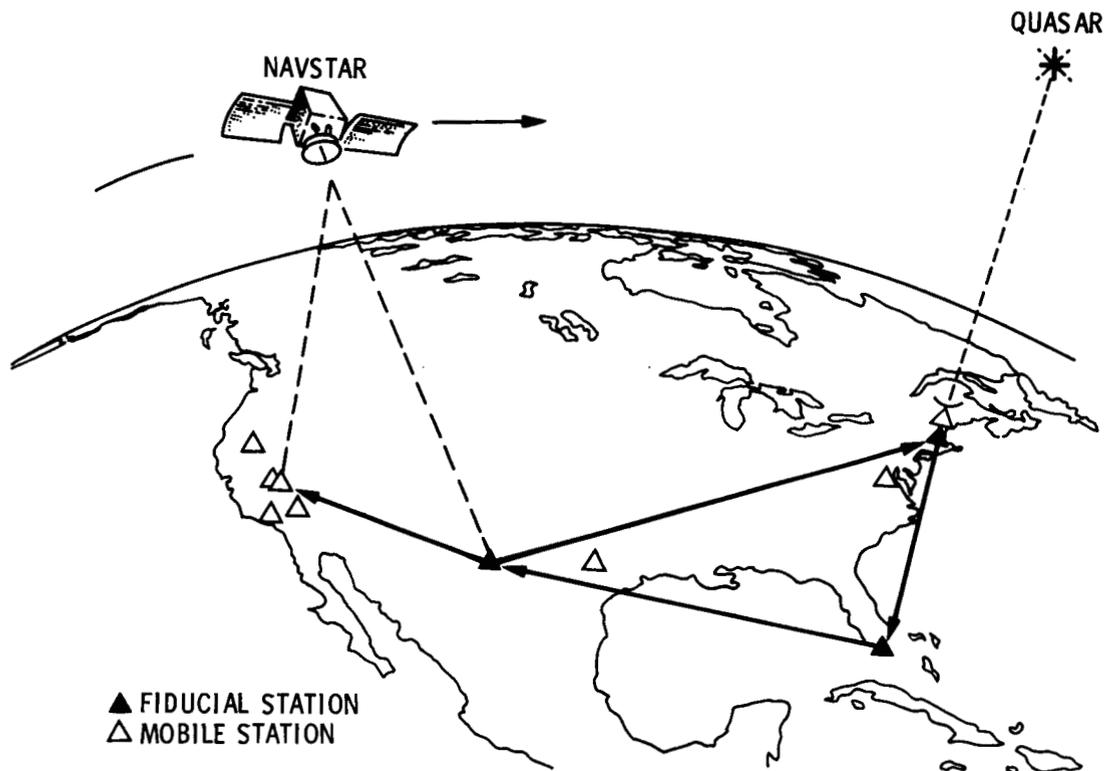
Figure 1. A schematic picture of North America as it would appear from a GPS satellite passing over the Galapagos Islands is shown. The sites to which mobile and fiducial receivers were deployed during the Spring 1985 HPBT are denoted by open and closed triangles, respectively.
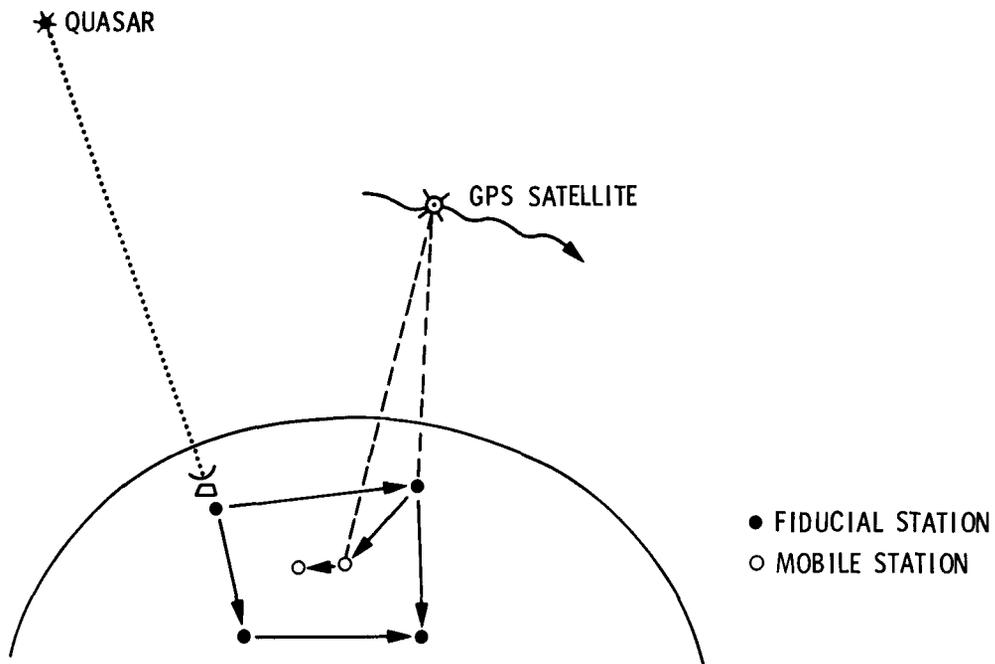
Figure 2. A schematic illustration of the fiducial network approach for GPS-based geodesy is shown. The fiducial station data enable the simultaneous estimation of GPS satellite orbits and mobile station locations. VLBI observations establish accurate fiducial station baselines and tie the GPS results to the inertial frame of the quasars.
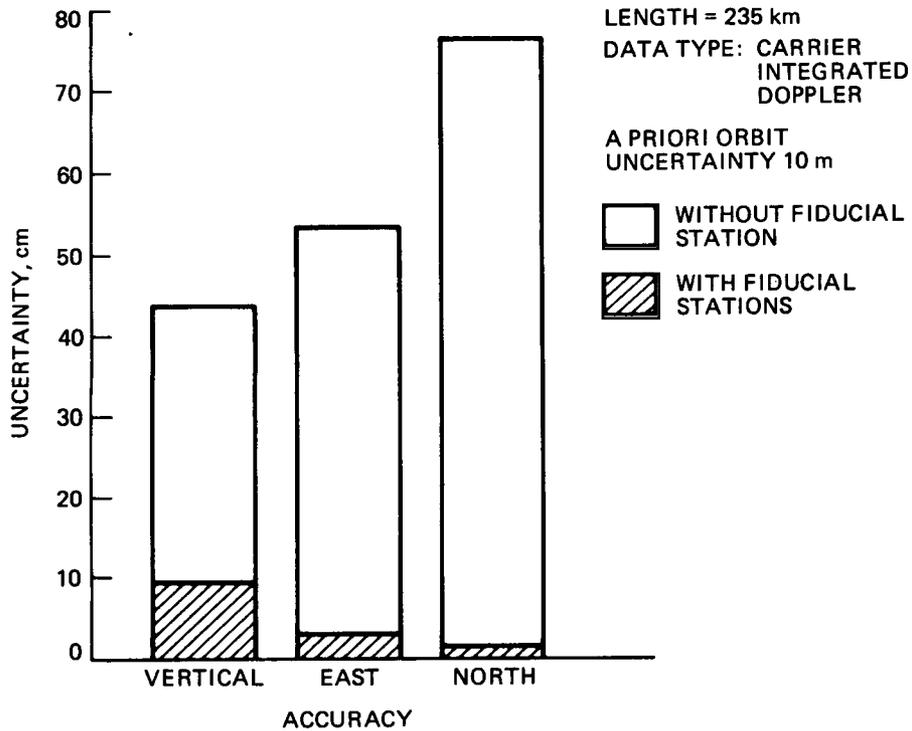
Figure 3. Covariance analysis results show expected baseline accuracies from the Spring 1985 HPBT for the Mojave/Owens Valley baseline. Results for two scenarios are displayed, illustrating the expected improvement in accuracy resulting from utilization of the fiducial network approach.

RMS (N) = 0.6 cm

RMS (E) = 2.4 cm

NORTH (cm)

5

0

+ VLBI

LENGTH = 245 km

-5   · 0   5

EAST (cm)
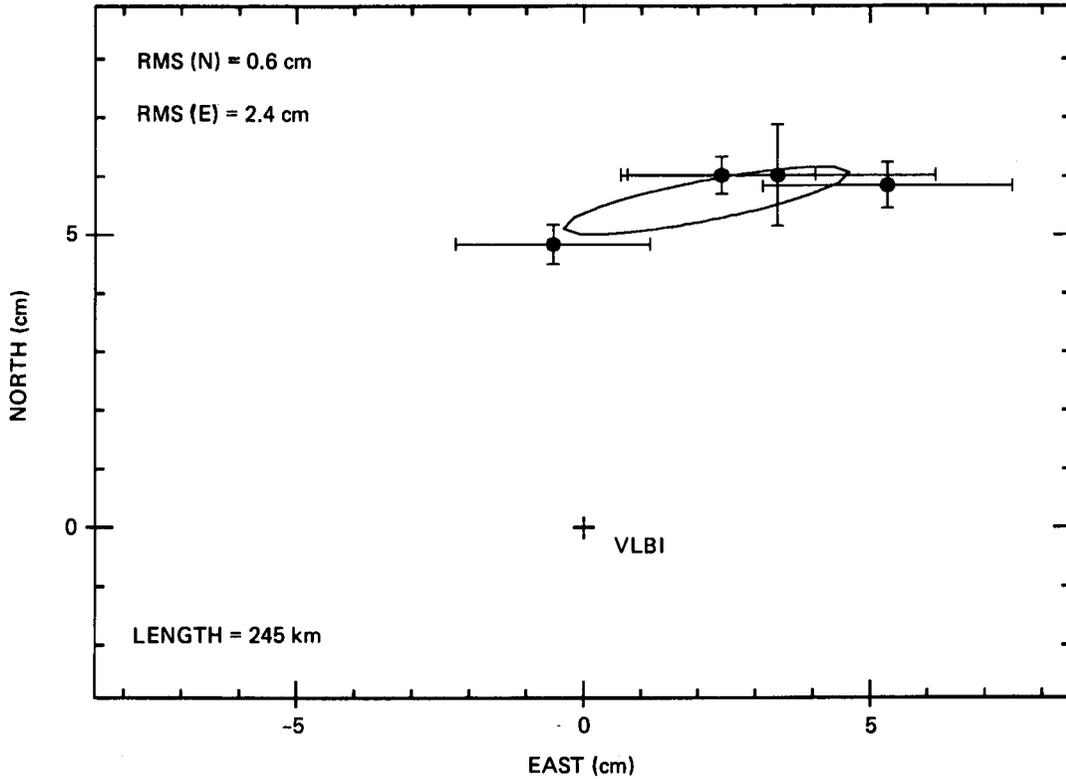
Figure 4. Day-to-day repeatability and comparison to colocated VLBI for
the OVRO/Mojave baseline between the two SERIES-X receivers is shown. Repeat-
ability about the mean in the north is 0.6 cm (RMS), or $3:10^7$, while in the
east it is $1:10^7$. The GPS-based result differs by about 6 cm, or $2:10^7$ in
the horizontal plane from the colocated VLBI measurement. This difference is
larger than can be readily explained and may be due to errors in the local
surveys correcting for the physical separations of the GPS and VLBI antennas.

RMS SCATTER (cm)

5

0

1:10^7

5:10^8

500 1000

BASELINE LENGTH (km)
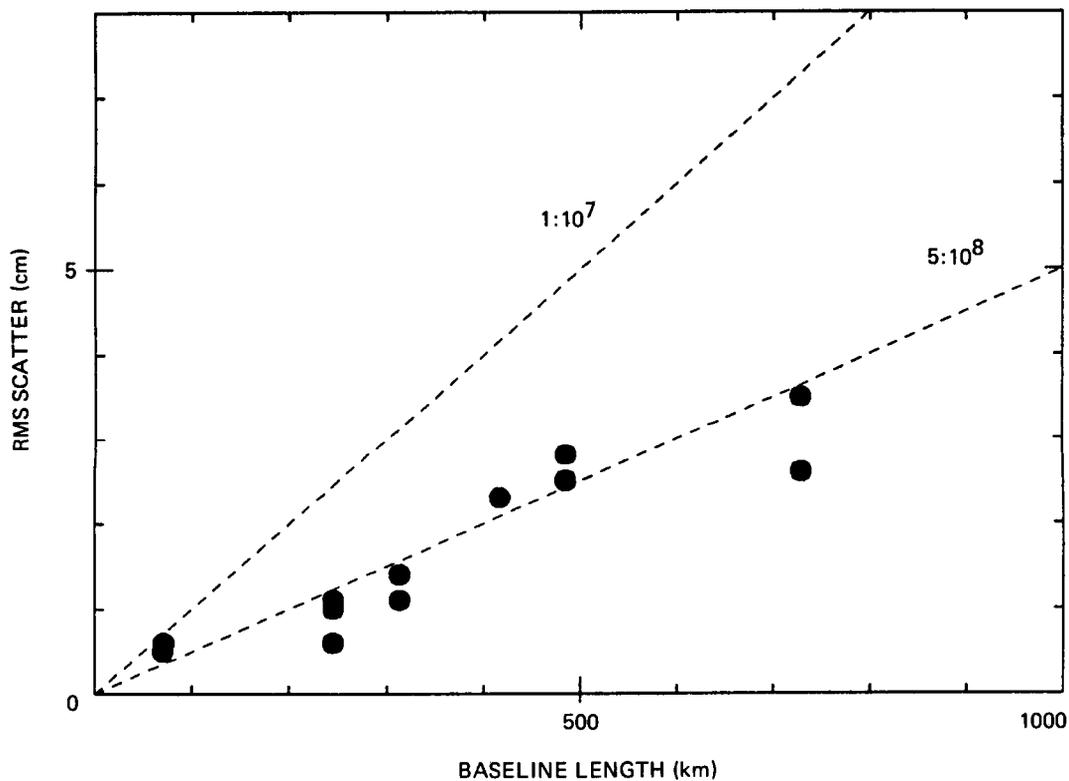
Figure 5. The day-to-day RMS repeatability about the mean of the north component is shown for all baselines connecting the receivers at the Mojave, OVRO, Hat Creek and Mammoth Lakes sites. This repeatability consistently falls near 10^8, or better, for all of these baselines, which range in length from 70 km to 729 km.
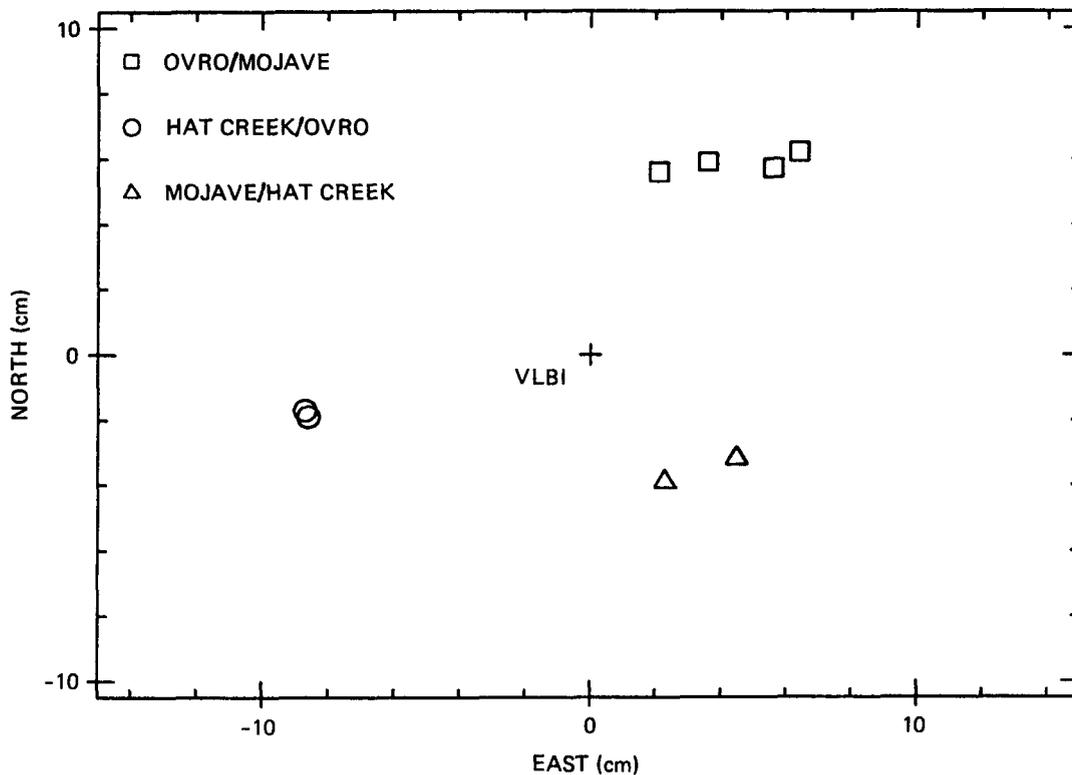
Figure 6. Differences between colocated GPS and VLBI measurement are shown for the eight baselines connecting the five receivers located at the Mojave, OVRO and Hat Creek sites. (See Table 2.) The systematic grouping of results by station pairs strongly suggests the presence of local survey errors.
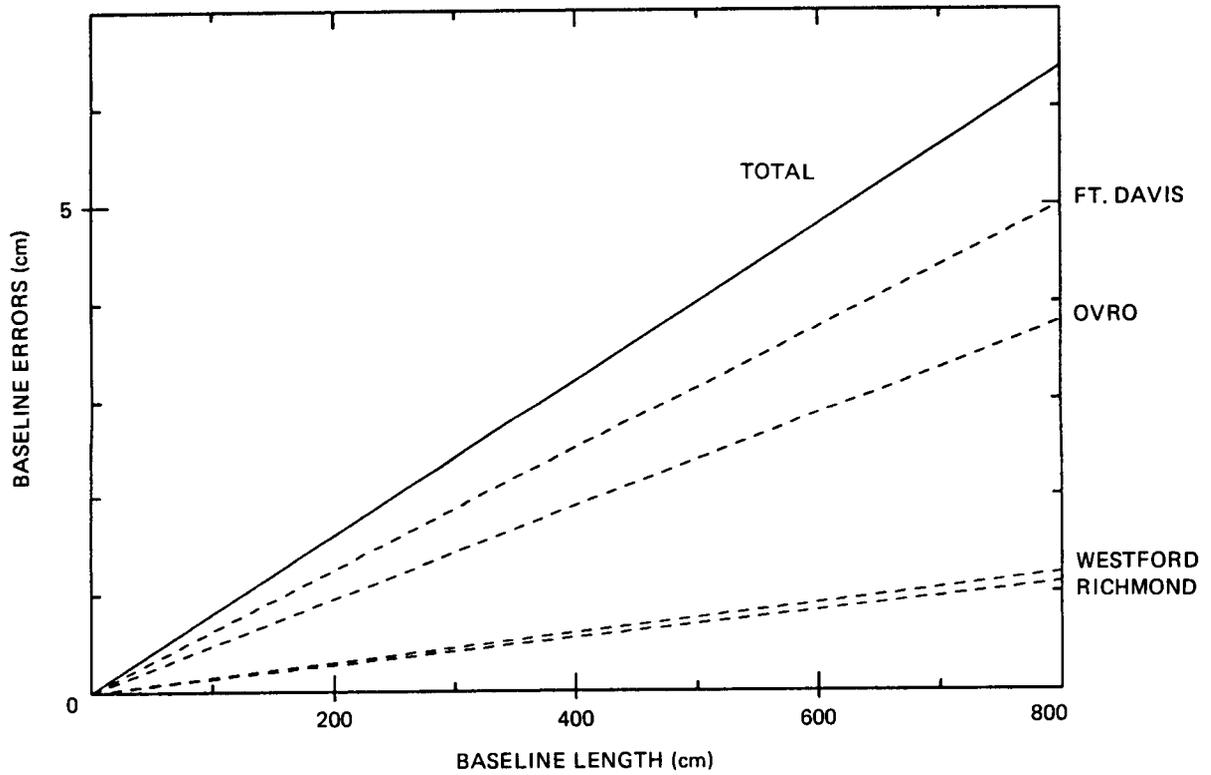
Figure 7. Consider error (RSS of all three components; see Section VI) in the mobile baselines, resulting from fiducial station location error, as a function of mobile baseline length is shown for the Spring 1985 HPBT. An uncertainty of 4 cm was assumed in each coordinate for each of the four fiducial receivers.
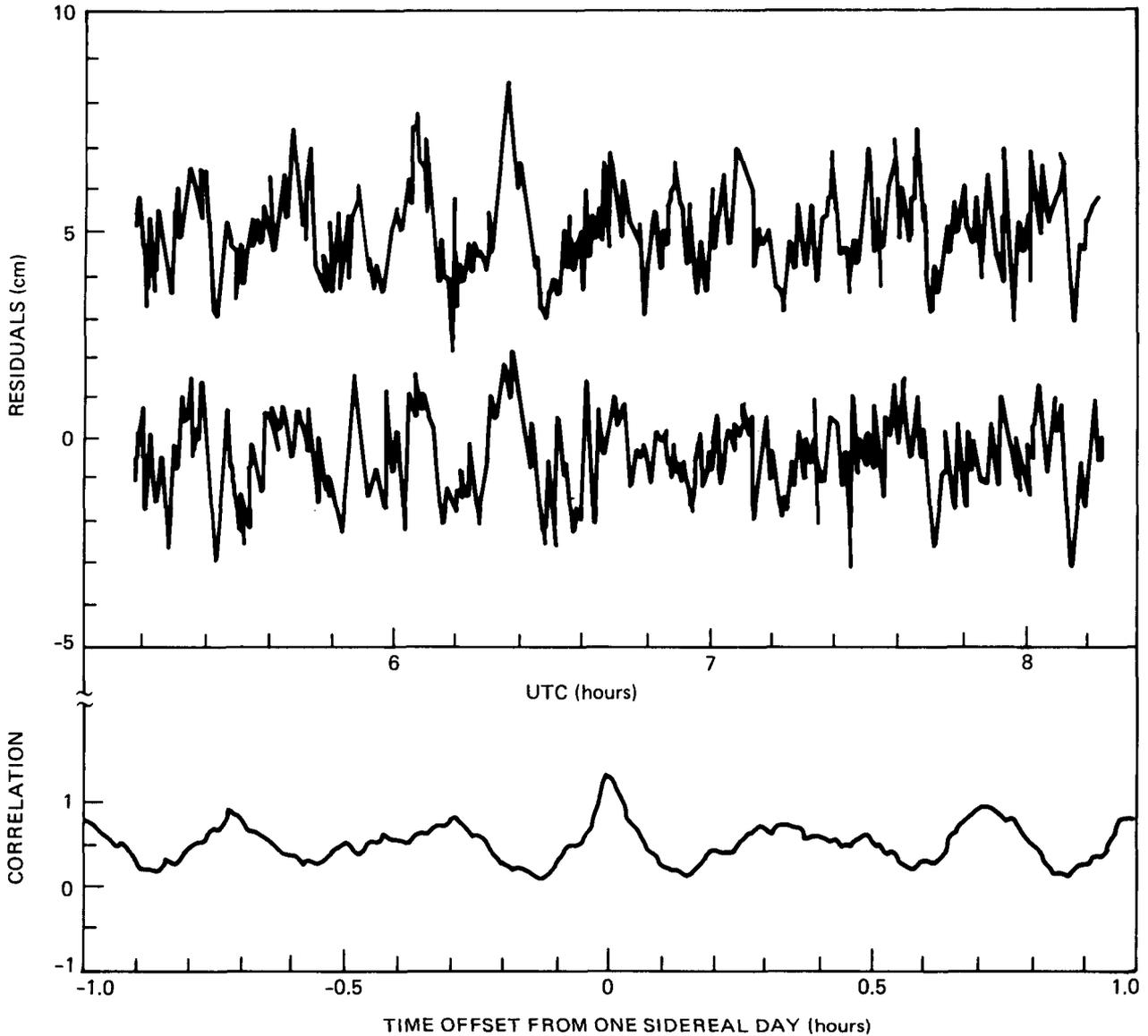
Figure 8. Post-fit residuals and cross-correlations for the TI-4100 carrier phase data of April 3 and 4, 1985, are shown. These data have been meteorologically and ionospherically calibrated, double-differenced (GPS 6 and GPS 8 transmitters, Mojave and OVRO receivers), and fitted to a tenth-order polynomial. Multipath error will be periodic on a sidereal day, resulting in correlation between the upper and lower plots. The high correlation for an offset of exactly one sidereal day indicates substantial multipathing error for the TI-4100 antenna.

61
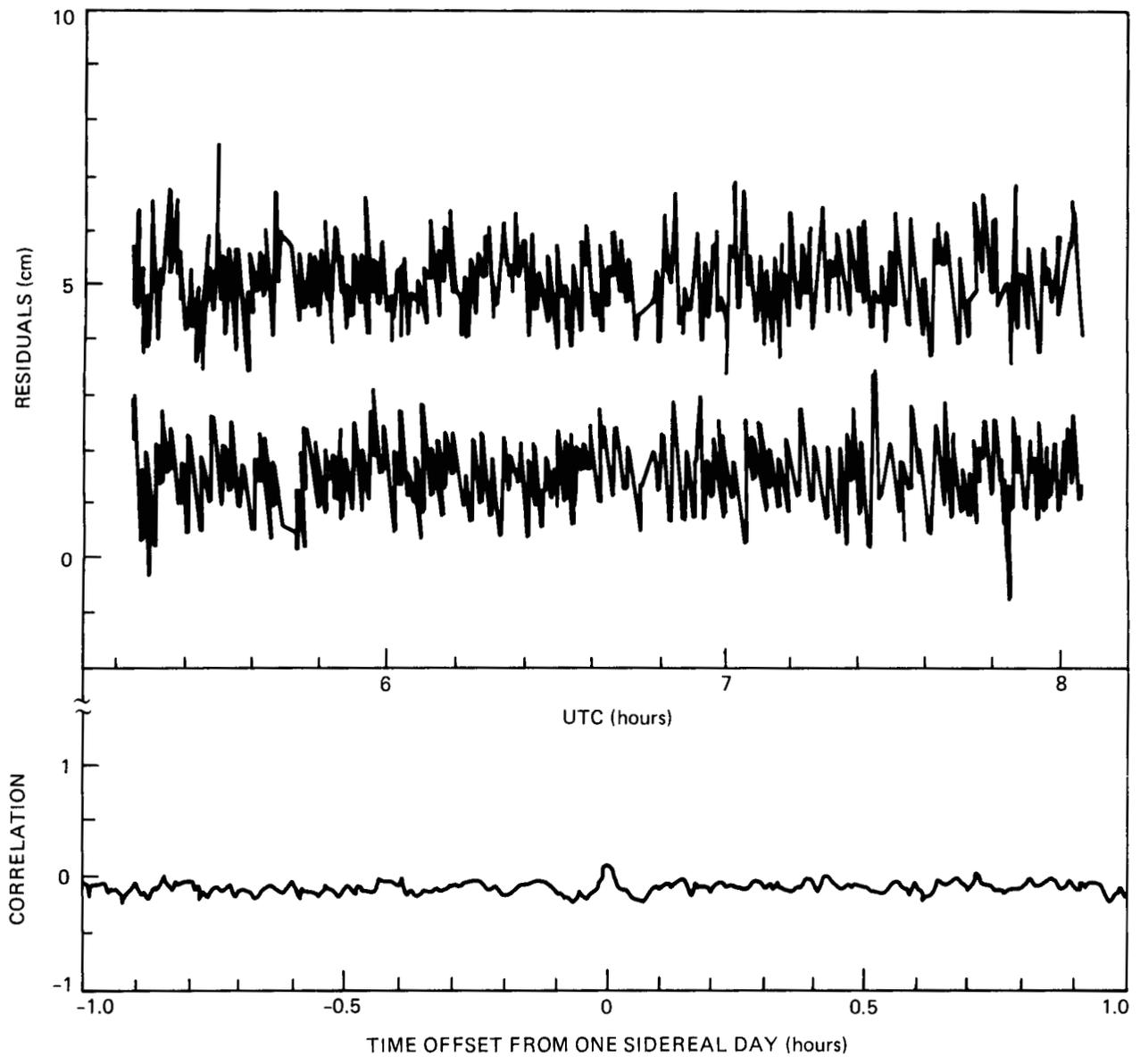
Figure 9. Post-fit residuals and cross correlations for the SERIES-X carrier phase data of April 3 and 4, 1985, are shown. These data have been treated as described in the caption for Figure 8. The small correlation for an offset of exactly one sidereal day indicates relatively small multipath error for the SERIES-X antennas.
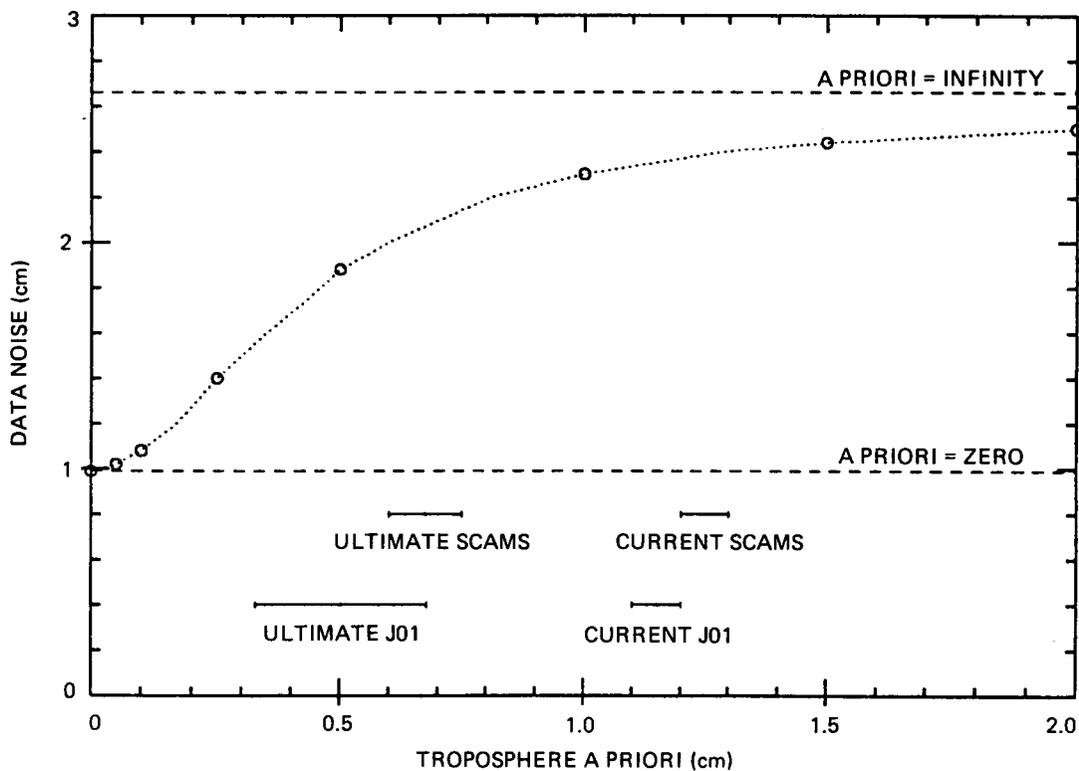
Figure 10. The formal error in the vertical baseline component for the Mojave/OVRO baseline, between TI-4100 receivers, is shown as a function of troposphere a priori uncertainty. Also shown are the current and ultimate calibration accuracies for two of the WVR models currently in use in JPL's GPS field exercises [S. E. Robinson, personal communication, 1987]. From this plot, we infer that in the case of the Spring 1985 HPBT, external troposphere calibration data contributed little to the precision of estimated vertical baseline components. (See Section VI.)
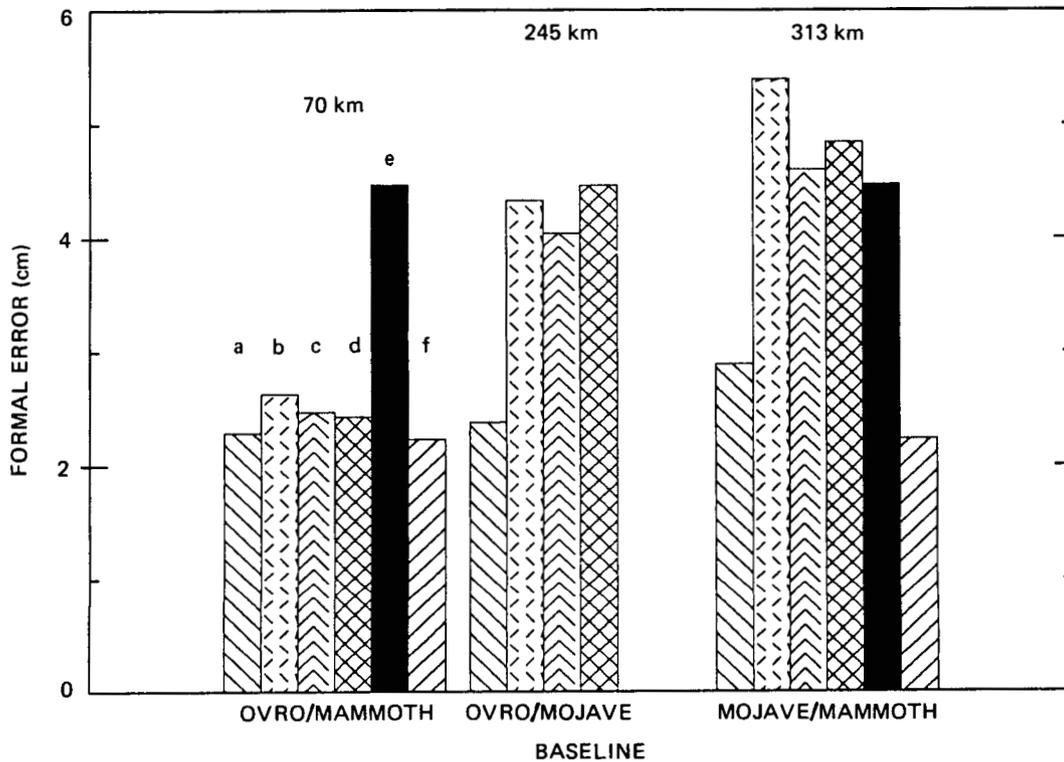
Figure 11. The formal errors in the north for the OVRO/Mammoth (70 km), OVRO/Mojave (245 km) and Mojave/Mammoth (313 km) baselines are shown for a variety of hypothetical fiducial outage scenarios. These include single-station outages at Westford, Richmond and Ft. Davis (cases b, c and d) and a two-station outage involving Westford and Richmond (case e). In the latter case, Ft. Davis, Mojave and OVRO are used as a more localized fiducial network. The formal errors for the standard case of a four-station fiducial network (with no outages) of Westford, Richmond, Ft. Davis and OVRO are shown as case a, and the formal errors for the five-station fiducial network, which includes the above stations plus Mojave, are shown as case f.
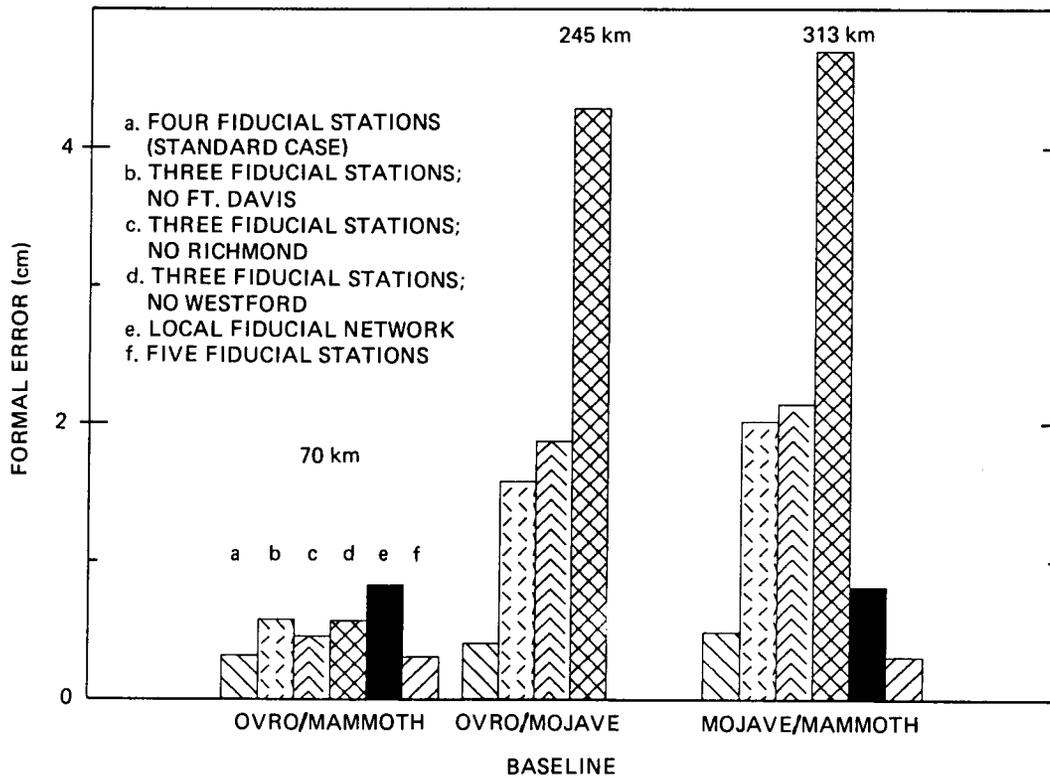
Figure 12. The formal errors in the east for the OVRO/Mammoth (70 km), OVRO/Mojave (245 km) and Mojave/Mammoth (313 km) baselines are shown for a variety of hypothetical fiducial outage scenarios. The case designations have the same meaning as in Figure 11.
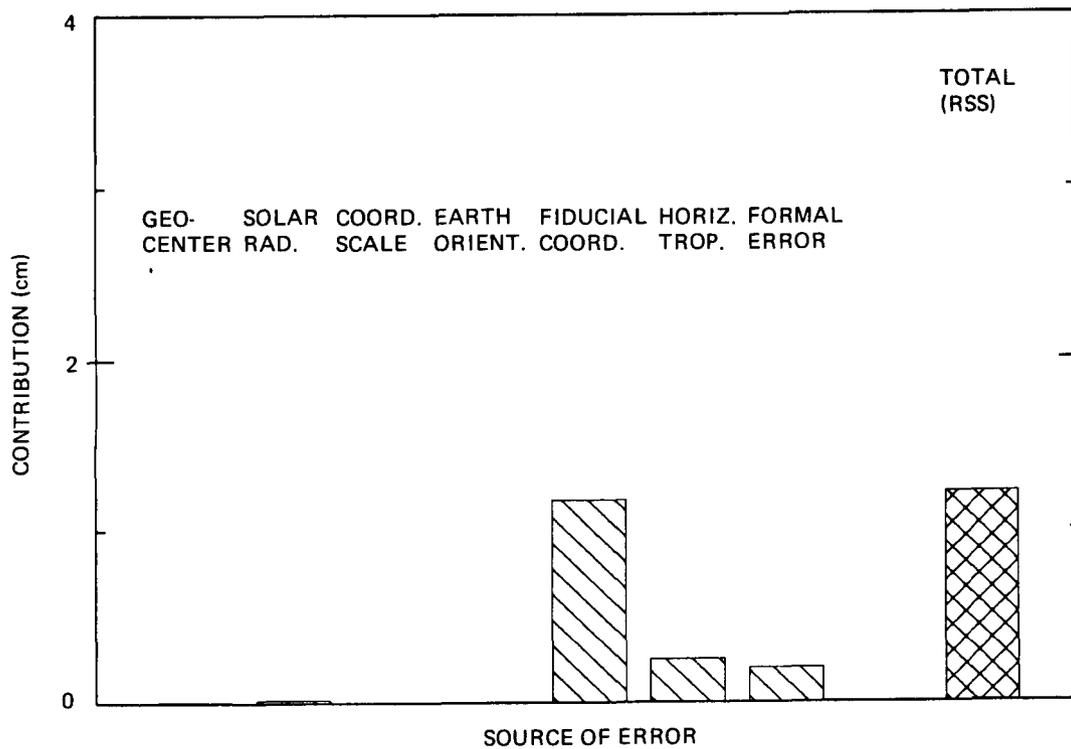
Figure 13. The total error budget for the north component of the 245 km OVRO/Mojave baseline between the SERIES-X receivers is shown. This error budget includes the contributions from all significant error sources, including consider errors, modeling errors in estimated parameters, and random, or formal, errors.
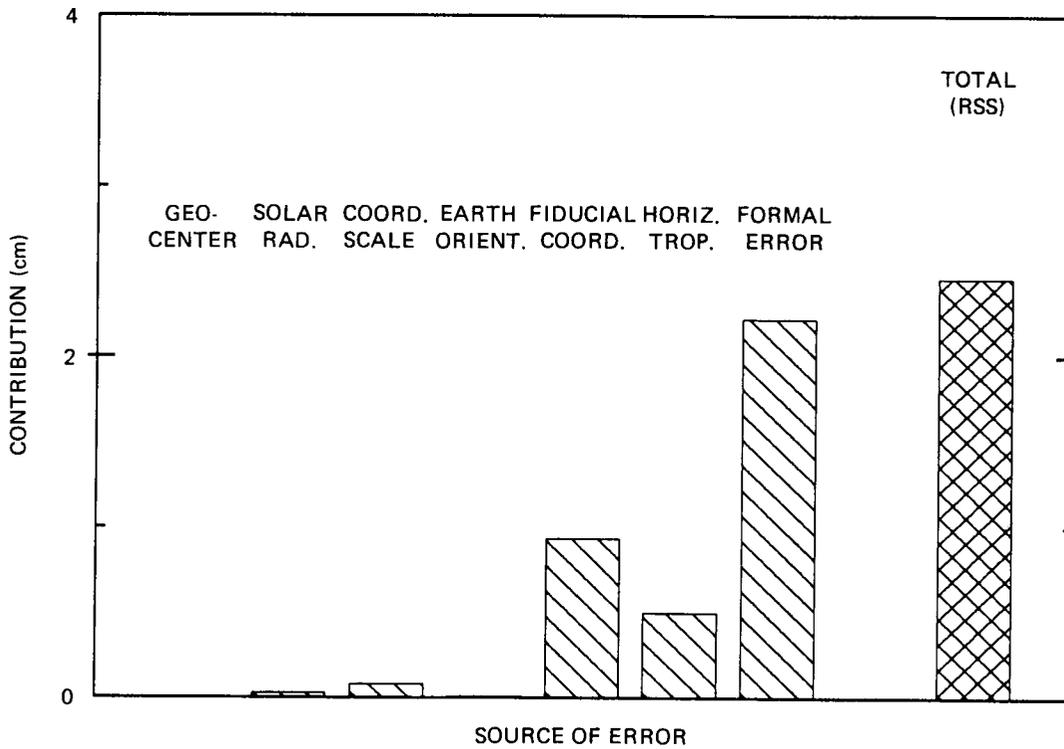
Figure 14.   The total error budget for the east component of the 245 km

OVRO/Mojave baseline between the SERIES-X receivers is shown.   This error

budget includes contributions as noted for Figure 13.

1. Report No. 87-35	2. Government Accession No.	3. Recipient's Catalog No.

4. Title and Subtitle
The Spring 1985 High Precision Baseline Test of the JPL GPS-Based Geodetic System A Final Report

5. Report Date
November 15, 1987

6. Performing Organization Code

7. Author(s) John M. Davidson, Catherine L. Thornton, Scott A. Stephens, Geoffrey Blewitt, Stephen M. Lichen,

8. Performing Organization Report No. *

9. Performing Organization Name and Address

JET PROPULSION LABORATORY
California Institute of Technology
4800 Oak Grove Drive
Pasadena, California 91109

10. Work Unit No.

11. Contract or Grant No.
NAS7-918

13. Type of Report and Period Covered
External Report
JPL Publication

12. Sponsoring Agency Name and Address

NATIONAL AERONAUTICS AND SPACE ADMINISTRATION
Washington, D.C. 20546

14. Sponsoring Agency Code
RE4 BP-676-59-31-20-30

16. Abstract

The Spring 1985 High Precision Baseline Test (HPBT) of the JPL GPS-Based Geodetic Measuring System was conducted between March 28, 1985, and April 5, 1985. It involved over a dozen collaborating institutions, with organization and coordination under NASA/JPL leadership, and was designed to meet a number of objectives. Foremost among these was the demonstration of a level of accuracy of $1\text{-}2{:}10^7$, or better, for baselines ranging in length up to several hundreds of kilometers.

These objectives were all met with a high degree of success, with respect to the demonstration of system accuracy in particular. The results from six baselines ranging in length from 70 to 729 km were examined for repeatability and, in the case of three baselines, were compared to results from colocated VLBI systems. Repeatability was found to be $5{:}10^8$ (RMS) for the north baseline coordinate, independent of baseline length, while for the east coordinate RMS repeatability was found to be larger than this by factors of 2-4. The GPS-based results were found to be in agreement with those from colocated VLBI measurements, when corrected for the physical separations of the VLBI and GPS antennas (typically on the order of 0.5 km), at the level of $1\text{-}2{:}10^7$ in all coordinates, independent of baseline length. The results for baseline repeatability are consistent with the current GPS error budget, but the GPS-VLBI intercomparisons disagree at a somewhat larger level than expected. We hypothesize that these differences may result from errors in the local survey measurements used to correct for the separations of the GPS and VLBI antenna reference centers.

17. Key Words (Selected by Author(s))

Geodesy; Geophysics

18. Distribution Statement

Unclassified; unlimited

19. Security Classif. (of this report) Unclassified	20. Security Classif. (of this page) Unclassified	21. No. of Pages	22. Price